14-3-3ζ regulates lipolysis by influencing adipocyte maturity

Abel Oppong[1,2], Kadidia Diallo[1,2], Isabelle Robillard Frayne[3], Christine Des Rosiers[3,4], Gareth E. Lim[1,2*]

[1]Department of Medicine, Université of Montréal, Montréal, QC, Canada

[2]Cardiometabolic axis, Centre de recherche de Centre hospitalier de l'Université de Montréal, Montréal, QC

[3]Montreal Heart Institute, Research Center, Montréal, QC, Canada

[4]Department of Nutrition, Université of Montréal, Montréal, QC, Canada

Running title: 14-3-3ζ regulates lipolysis through adipocyte maturity

Keywords: Scaffold proteins, adipocyte, heterogeneity

***To whom correspondence should be address:** Gareth E. Lim, CRCHUM, Tour Viger, Rm 08.482, 900 Rue St. Denis, Montréal, QC H2X 029, Canada; gareth.lim@umontreal.ca; Tel: (514) 890-8000 ext 12927

Disclosure statement: The authors have nothing to disclose.

Keywords: adipocyte, 14-3-3ζ, scaffold, lipase, maturity

Abbreviations: ATGL, adipose triacylglycerol lipase; HSL, hormone-sensitive lipase; MAGL, monoacylglycerol lipase; PKA, protein kinase A; cAMP, cyclic adenosine monophosphate

Abstract

Activation of β3-adrenergic receptors on mouse adipocytes promotes lipolysis, or the catabolism of stored lipids, via the concerted actions of PKA and lipases, including HSL, ATGL, and MAGL. Phosphorylation of HSL by PKA generates phospho-binding sites for 14-3-3 proteins, a ubiquitously expressed family of molecular scaffolds, of which we previously identified essential roles of the 14-3-3ζ isoform in murine adipogenesis. The presence of 14-3-3ζ binding sites on HSL and ATGL suggests that 14-3-3ζ may influence their activities and ultimately lipolysis. Herein, we demonstrate that 14-3-3ζ is necessary for lipolysis in male mice, as deletion of 14-3-3ζ in adipocytes was found to impair glycerol and FFA release. 14-3-3ζ was found to be heterogeneously expressed among adipocytes in gonadal white adipose tissue (gWAT), and deletion of 14-3-3ζ significantly decreased the number of small (<200μm) adipocytes. Adipocyte-specific deletion of 14-3-3ζ also reduced PPARγ and HSL protein abundance and significantly reduced the expression of genes associated with adipocyte maturity. Similarly, depletion of 14-3-3ζ in mature 3T3-L1 adipocytes impaired lipolysis, and as with primary mouse adipocytes, reducing 14-3-3ζ abundance decreased the expression of mature adipocyte genes. Moreover, depletion of 14-3-3ζ promoted the acquisition of a lipidomic signature that resembled undifferentiated, immature 3T3-L1 cells. Collectively, these findings reveal a novel role for 14-3-3ζ in regulating PKA-dependent lipolysis, potentially by controlling the adipocyte maturity.

Introduction

The primary function of white adipose tissue (WAT) is to regulate energy and nutrient homeostasis, as white adipocytes specialize in both the storage of triacylglycerols (TAGs) and the mobilization of free fatty acids (FFAs). These processes occur to accommodate changes in metabolic demand during periods of activity or fasting [1]. In WAT, FFAs are generated by the hydrolysis of TAGs through a process known as lipolysis, which occurs following the binding of catecholamines to β3-adrenergic receptors, the subsequent generation of the second messenger, cAMP, and the activation of Protein Kinase A (PKA) [1]. TAG hydrolysis is principally mediated by PKA-dependent phosphorylation of three lipases: adipose triacylglycerol lipase (ATGL), hormone-sensitive lipase (HSL), and monoacylglycerol lipase (MAGL), whereby they respectively catalyze the sequential conversion of TAGs into diacylglycerols (DAGs), monoacylglycerols (MAGs), and finally FFAs and glycerol [2, 3].

Molecular scaffolds belonging to the 14-3-3 family are ubiquitously expressed proteins that have been implicated in regulating cellular processes, such as proliferation, apoptosis and metabolism [4-6]. These functions arise from their ability to interact with target proteins harboring specific phosphorylated serine and threonine motifs [7, 8]. For example, the inhibitory actions of the Rab-GAP, AS160/TBC1D4, on GLUT4 translocation are attenuated following its interactions with 14-3-3 proteins [9], and interactions with FOXO1 retains this transcription factor in the cytoplasm [10]. We previously reported essential roles of one of the seven mammalian isoforms, 14-3-3ζ, in adipogenesis, as systemic deletion of 14-3-3ζ in mice resulted in significant reductions in visceral adipose tissue mass and decreased expression of mature adipocyte markers in gonadal adipocytes [6]. Furthermore, through the use of proteomics to elucidate the 14-3-3ζ interactome, we found that 14-3-3ζ may influence RNA splicing and processing during adipocyte development [11]. However, whether 14-3-3ζ has functions specific to mature adipocytes has not been fully examined.

One of the earliest reported functions of 14-3-3 proteins is their regulatory functions on tyrosine and tryptophan hydroxylases, which accounts for their alternative names of tyrosine 3-monooxygenase/tryptophan 5-monooxygenase activation proteins [12], and given their ability to bind to proteins harboring specific serine or threonine motifs they can interact and regulate a diverse array of enzymes to influence intracellular signaling pathways. For example, the activity of other kinases, such as PKA and RAF-1, are positively regulated upon binding to 14-3-3 proteins, but in some instances, inhibitory effects, as seen with DYRK1A, have been reported [13-15]. The presence of 14-3-3 protein binding motifs generated by PKA phosphorylation on either ATGL and

HSL has been reported, which that 14-3-3 proteins could have regulatory roles in lipolysis [16]. Thus, we turned our focus to examining the potential contributions of 14-3-3ζ to lipolysis.

Herein, we report that 14-3-3ζ is necessary for lipolysis in mature adipocytes, as adipocyte-specific deletion of 14-3-3ζ in mice and siRNA-mediated depletion of 14-3-3ζ in mature 3T3-L1 adipocytes impaired glycerol and free fatty acid release. Although reductions in 14-3-3ζ was found to affect distal events in the lipolytic pathway, we report on an unexpected role of 14-3-3ζ in the regulation of adipocyte maturity. Reductions in 14-3-3ζ expression were associated with decreased mRNA and protein levels for key markers of mature adipocytes, including *Pparg*/PPARγ, *Hsl*/HSL, and *Atgl*/ATGL. Moreover, decreased mRNA levels for genes involved in *de novo* triglyceride synthesis and fatty acid transport was observed. Depletion of 14-3-3ζ was also found to alter the lipidome by promoting the acquisition of a lipid signature resembling pre-adipocytes. In conclusion, this study identifies critical roles of 14-3-3ζ in the function of mature adipocytes and reports a novel function of 14-3-3ζ in the regulation of adipocyte maturity.

Materials and Methods

Animal husbandry

Adipoq-CreERT2^{Soff} mice (stock no. 025124, JAX, Bar Harbor Maine) were bred with *Ywhaz*$^{flox/flox}$ mice harboring LoxP sites that flank exon 4 of *Ywhaz* (gene that encodes 14-3-3ζ) (Ywhaz$^{tm1c(EUCOMM)HMgu}$, Toronto Centre for Phenogenomics, Toronto, Canada) to generate *Adipoq*-CreERT2-14-3-3ζKO mice (adi14-3-3ζKO) [17]. Both strains were on a C57Bl/6J background. To delete exon 4 of *Ywhaz,* tamoxifen (TMX, 50 mg/kg b.w; Sigma Aldrich, St. Louis, MO) was administered by intraperitoneal injections for five days (Figure 1A). Transgenic mice over-expressing a TAP-tagged human 14-3-3ζ molecule were on a CD1 background and were provided by the laboratory of Dr. Amparo Acker-Palmer [6, 18]. All mice were maintained on a standard chow diet (Teklad diet no. TD2918) under 12-hour light/12-hour dark cycles in an environmentally controlled setting (22°C ± 1°C) with free access to food and water. All procedures were approved and performed in accordance with CIPA (Comité institutionnel de protection des animaux du CRCHUM) guidelines at the University of Montreal Hospital Research Centre.

Metabolic phenotyping

For glucose tolerance tests, adi14-3-3ζKO mice were fasted for six hours and challenged with d-glucose (2 g/kg b.w.; VWR, Solon, OH) by intraperitoneal administration [6, 19]. For insulin tolerance tests, adi14-3-3ζKO mice were fasted for four hours and were injected intraperitoneally with Humulin R insulin (0.5 U/kg b.w; Eli Lilly, Toronto, ON) [6, 19]. Blood glucose was measured from tail blood with a Contour Next EZ glucose meter (Ascencia Diabetes Care, Basel, Switzerland). Plasma leptin, insulin, and adipocnectin were measured by ELISA (ALPCO, Keewatin, NH) according to the manufacturer's protocols.

Cell Culture and transient transfections

3T3-L1 cells were maintained in DMEM (Life Technologies Corporation, Grand Island, NY), supplemented with 10% newborn calf serum (NBCS) and 1% penicillin/streptomycin (P/S) and were seeded onto 12-well plates (100,000 cells/well) or 10cm dishes ($2x10^6$ cells/dish) 2 days prior to the induction of differentiation. Confluent cells were treated with a differentiation cocktail (DMEM supplemented with 10% FBS, 1% P/S, 500 µM IBMX, 500 nM dexamethasone and 172 nM insulin) for 48 hours, followed by media replacement (DMEM with 10% FBS, 1% P/S and 172 nM insulin) every 2 days for 7-8 days [6, 11]. Knockdown

and overexpression of 14-3-3ζ was achieved by transfecting day 7-8 differentiated cells with scrambled control siRNA, 14-3-3ζ-specific siRNA (Ambion, Austin, TX), GFP control plasmids, or plasmids encoding 14-3-3ζ (14-3-3ζ IRES-GFP) using the Amaxa Cell Line Nucleofector Kit L, as per manufacturer's instructions (Lonza, Koln, Germany). Differentiated 3T3-L1 cells were stained with Oil Red-O (ORO) and measured, as previously described [6, 11]. All studies with 3T3-L1 cells were performed on cells between passages 10-16.

Measurements of lipolysis

Adi14-3-3ζKO mice were injected with 1 mg/kg CL-316,243 (Sigma-Aldrich, St. Louis, MO) following an overnight fast. TAP mice were injected with 10 mg/kg isoproterenol (Sigma-Aldrich), following an overnight fast. Blood was collected from the tail vein before and 30 minutes after administration of CL-316,243 or isoproterenol. To measure lipolysis *ex vivo,* mice where sacrificed 4 weeks after the last TMX injection, and gonadal adipose tissues were harvested and placed into pH 7.4-adjusted Krebs-Ringer buffer (135 mM NaCl, 3.6 mM KCl, 0.5 mM NaH_2PO_4, 0.5 mM $MgCl_2$, and 1.5 mM $CaCl_2$), supplemented with 10 mM HEPES, 2 mM $NaHCO_3$, 5 mM glucose and 2% bovine serum albumin (BSA). Gonadal explants were treated with or without 1 μM isoproterenol (Sigma Aldrich) for two hours. The supernatant was collected and centrifuged for 15 minutes at 1500 RPM. To measure lipolysis from differentiated 3T3-L1 cells (Zenbio, Research Triangle Park, NC), cells were incubated in starvation media consisting of pH 7.4-adjusted Krebs-Ringer buffer, 5 mM glucose and 0.2% BSA for two hours. Cells were then incubated in experimental media consisting of pH 7.4-adjusted Krebs-Ringer buffer, 5 mM glucose and 2% BSA for two hours while treated with 1 μM isoproterenol (Sigma-Aldrich), 10 μM forskolin with 0.5 mM IBMX (Sigma-Aldrich), or 1 mM dibutyryl cAMP (Sigma-Aldrich). Lipolysis was assessed by measuring glycerol and free fatty acid (FFA) levels using triglyceride (Sigma-Aldrich) and non-esterified fatty acid (NEFA; Wako Diagnostics, Osaka, Japan) kits, as per the manufacturer's protocol.

RNA isolation and qPCR

After 48 hours, total RNA was isolated from differentiated 3T3-L1 cells using the RNeasy kit (Qiagen, Hilden, Germany). cDNA was generated using the High-Capacity cDNA Reverse Transcription kit (ThermoFisher Scientific, Waltham, MA). Measurements of mRNA were performed with SYBR green chemistry using the QuantStudio 6-flex Real-time PCR System (ThermoFisher Scientific). All data were normalized to either *Hprt* or *Actinb* by the ΔC(t) method [6, 11]. Primer sequences are listed in Supplemental Table 1.

Measurement of intracellular cAMP levels

After 7 days of differentiation, mature 3T3-L1 adipocytes were transfected with scrambled, control siRNA (siCon) or siRNA against 14-3-3ζ (si14-3-3ζ). After 48 hours, cells were incubated in starvation media (pH 7.4-adjusted Krebs-Ringer buffer, 5 mM glucose, and 0.2% BSA) for two hours, followed by incubation in experimental media in the presence of 1 μM Isoproterenol or 20 μM forskolin with 0.5 mM IBMX for one hour. Lysates were harvested and intracellular cAMP levels were assayed using the cAMP Parameter Assay Kit (R&D Systems, Minneapolis, MN).

Immunoblotting and immunohistochemistry

Differentiated 3T3-L1 cells were lysed in RIPA buffer (0.9% NaCl, 1% v/v triton X-100, 0.5% sodium deoxycholate, 0.1% SDS, and 0.6% tris base) supplemented with protease and phosphatase inhibitors (Sigma-Aldrich). Proteins were resolved by SDS-PAGE and transferred to PVDF membranes, as previously described [6, 11]. Gonadal and inguinal adipose tissues were harvested from WT and adi14-3-3ζKO mice, fixed in 4% paraformaldehyde (Sigma-Aldrich), embedded in paraffin, and sectioned to 6 μm thickness. Immunohistochemistry for perilipin (Cell Signaling Technology, Danvers, MA) or perilipin (Fitzgerald, Acton, MA) and 14-3-3ζ (Abcam, Toronto, ON) was performed with established protocols, and Cell Profiler (3.0.0) was used to determine adipocyte size, as previously described [6, 20]. To image lipid droplets, mature 3T3-L1 adipocytes were seeded in chamber slides (ThermoFisher Scientific) coated with Poly-D-lysine (Sigma-Aldrich) after electroporation with either a scrambled, control (siCon) or siRNA against 14-3-3ζ, and cells will incubated with 0.5 μm Hoechst 33342 and 2 μm Bodipy 493/503 (ThermoFisher Scientific). Following successive washes with PBS, cells were fixed with 4% paraformaldehyde and cover-slipped after addition of ProLong Gold mounting medium (ThermoFisher Scientific). All images were taken with an Evos FL fluoresecent microscope (ThermoFisher Scientific). All antibodies and their concentrations are listed in Supplemental Table 2.

Untargeted lipidomic analysis (LC-MS)

Methanol fixed siRNA-transfected, differentiated 3T3-L1 cells were processed for lipid extraction and untargeted LC-MS lipidomics, as previously described [21]. In brief, samples (0.50 μl to 1.82 μl), spiked with six internal standards: LPC 13:0, PC19:0/19:0, PC14:0/14:0, PS12:0/12:0, PG15:0/15:0 and PE17:0/17:0 (Avanti Polar Lipids Inc, Alabaster, USA), were analyzed using a 1290 Infinity HPLC coupled with a 6530 Accurate Mass

Quadrupole-Time-of-Flight (QTOF) equipped with a dual ion spray electrosource (Agilent, Santa Clara, CA) and operated in the positive mode. Lipids are eluted on a Zorbax Eclipse plus column (C18, 2.1 x 100 mm, 1.8 µm, Agilent Technologies Inc.) over 83 minutes at 40 °C using a gradient of solvent A (0.2% formic acid and 10 mM ammonium formate in water) and B (0.2% formic acid and 5 mM ammonium formate in methanol/acetonitrile/methyl tert-butyl ether [MTBE], 55:35:10 [v/v/v]). MS data processing was achieved using Mass Hunter Qualitative Analysis software package (version B.06) and a bioinformatic script that we have developed and encoded in both Perl and R languages to enable optimal MS data alignment between runs. This yields a data set listing features with their mass (*m/z*), corrected signal intensity, and retention time. Lipid identification was achieved by alignment using an in-house reference database in which 498 lipids have previously been identified by MS/MS.

Statistical analyses

Data are expressed as mean ± standard error of the mean. Data were analyzed by one- or two-way ANOVA or Student's t-test. A p-value less than 0.05 was considered statistically significant. For lipidomic analysis, the output text file containing the processed data was imported into Mass Professional Pro software (version 12.6.1, Agilent Technologies Inc.) and independent testing of each feature was achieved using an unpaired student's *t*-test followed by Benjamini-Hochberg correction. For selecting features discriminating siCon- vs. si14-3-3ζ-transfected cells, we have applied a corrected *P*-value as an estimation of False Discovery Rate (FDR) of < 5%) and and a fold change (FC) >2 and <0.5.

Results

Adipocyte-specific deletion of 14-3-3ζ impairs lipolysis in mice

To investigate the *in vivo* contributions of 14-3-3ζ to lipolysis, we generated tamoxifen (TMX)-inducible, adipocyte-specific 14-3-3ζ knockout (adi14-3-3ζKO) mice whereby exon 4 of *Ywhaz* was deleted (Figure 1A). Quantitative PCR confirmed that *Ywhaz* expression was significantly decreased in gonadal white (gWAT) and inguinal white (iWAT) adipose tissues, and no effects on expression of the remaining 6 isoforms were detected (Figure 1B, Figure S1A). Following TMX treatment, no effects on body weights between adi14-3-3ζKO and Cre+ wild-type (WT) littermate controls were observed in male and female mice (Figure 1C, Figure S1B), and adipocyte-specific deletion of 14-3-3ζ did not affect glucose metabolism or insulin sensitivity, as determined by intraperitoneal glucose tolerance (IPGTT) and intraperitoneal insulin tolerance (ITT) tests (Figures 1D,E, Figure S1C,D). Additionally, no differences in circulating insulin were detected in male mice following 14-3-3ζ deletion in adipocytes (Figure 1F).

Given the presence of 14-3-3 protein binding sites in ATGL and HSL [16, 22], we sought to examine whether deletion of 14-3-3ζ in adipocytes would impact lipolysis. WT and adi14-3-3ζKO mice were fasted overnight and challenged with the β3-adrenergic agonist, CL-316,243. In male adi14-3-3ζKO mice, a significant reduction in plasma glycerol levels following intraperitoneal administration of CL-316,243 was detected (Figure 1G); however, no significant differences were observed in female adi14-3-3ζKO mice (Figure S1E). Our observation of impaired glycerol release in male adi14-3-3ζKO mice prompted us to further examine if the effect of 14-3-3ζ was specific to adipose tissue. Explant studies with gWAT were performed whereby gWAT from male WT and adi14-3-3ζKO mice were stimulated with isoproterenol, and significantly impaired isoproterenol-mediated FFA and glycerol release were detected from adi14-3-3ζKO gonadal white adipose tissue (gWAT) explants (Figure 1H). To examine the consequence of 14-3-3ζ over-expression on lipolysis, transgenic mice over-expressing a TAP-tagged human 14-3-3ζ molecule and WT littermate controls were injected with isoproterenol, and no differences were observed (Figure S2A,B). Collectively, these data demonstrate that only adipocyte-specific deletion of 14-3-3ζ is sufficient to impair lipolysis.

Adipocyte-specific deletion of 14-3-3ζ alters gonadal adipocyte size

We previously reported that systemic deletion of 14-3-3ζ in mice caused significant reductions in the size and mass gWAT [6]. However, it was not clear if these effects were specific to 14-3-3ζ deletion in

adipocytes. In the present study, no differences in average size or distribution of adipocytes in iWAT from adi14-3-3ζKO mice were observed (Figure 2A-C). In contrast, adipocytes within gWAT were significantly smaller, and decreases and increases in the relative proportion of smaller (<200 μm) and larger (>600 μm) were observed (Figure 2D-F). When taken together, these findings suggest that the predominant effect of 14-3-3ζ deletion may be restricted to adipocytes within visceral depots.

14-3-3ζ depletion impairs lipolysis in 3T3-L1 cells

To further understand how 14-3-3ζ could influence lipolysis, differentiated 3T3-L1 adipocytes were transfected with siRNA against 14-3-3ζ (Figure 3A,B). No off-target effects on the expression of the remaining 14-3-3 isoforms were detected (Figure 3C). To assess the impact on lipolysis, glycerol and FFA levels were measured in the supernatant of 14-3-3ζ-depleted 3T3-L1 adipocytes after the addition of lipolytic stimuli, and when compared to control cells (siCon), knockdown of 14-3-3ζ (si14-3-3ζ) significantly impaired lipolysis in response to isoproterenol, forskolin, and dibutyryl cAMP (dbcAMP) (Figure 3D). As each compound targets effectors at different points in the β3-adrenergic receptor pathway, these findings suggest that depletion of 14-3-3ζ affects a distal event that facilitates lipolysis. In contrast to what was observed with over-expression of 14-3-3ζ *in vivo*, transient transfection of mature 3T3-L1 adipocytes with plasmid to over-express 14-3-3ζ was associated with a potentiation in isoproterenol-mediated lipolysis (Figure S2C,D).

As 14-3-3ζ depletion impaired lipolysis, it prompted further examination of where within the β3-adrenergic signaling pathway was affected by 14-3-3ζ knockdown. We first looked at mRNA expression of the β-adrenergic receptor isoforms (*Adrb1, Adrb2,* and *Adrb3*) in mature, 14-3-3ζ-depleted 3T3-L1adipocytes. While there were no changes in mRNA levels for *Adrb1* and *Adrb2*, a significant reduction in *Adrb3* mRNA levels, which is mainly expressed in adipocytes [23], was observed (Figure 4A). The attenuation of forskolin-mediated lipolysis suggested that defects in adenylyl cyclase activity could be occurring following 14-3-3ζ depletion (Figure 3D). However, no differences in the abilities of isoproterenol or forskolin to stimulate cAMP production were observed (Figure 4C), nor were significant differences in the expression of various phosphodiesterases, which degrade cAMP, detected between groups (Figure 4B). Surprisingly, significant reductions in mRNA and protein levels of *Atgl*/ATGL and *Hsl*/HSL were detected in 14-3-3ζ depleted 3T3-L1 cells (Figure 4D,E), in addition to protein abundance of the PKA target, CREB (Figure 4E). Collectively, these findings suggest that 14-3-3ζ is

required for the proper expression and function of effectors within the β-adrenergic signaling pathway that controls lipolysis.

Deletion of 14-3-3ζ in primary white adipocytes reduces the expression of mature adipocyte markers

To examine whether 14-3-3ζ deletion could also reduce the expression of lipases in primary adipocytes, quantitative PCR and immunoblotting was performed. Unlike what was observed in 3T3-L1 cells, mRNA levels of *Atgl* and *Hsl* were not affected by deletion of 14-3-3ζ (Figure 5A,B). Immunoblotting for HSL revealed marked reductions in protein abundance in gWAT from adi14-3-3ζKO mice (Figure 5D). Moreover, PPARγ2 protein abundance was reduced in gWAT from adi14-3-3ζKO mice was detected, which suggests a loss of adipocyte identity or maturity (Figure 5D). No differences in total TAGs were observed in gWAT or iWAT from WT and adi14-3-3ζKO mice (Figure 5E), but genes associated with *de novo* triglyceride synthesis were significantly reduced only in gWAT of adi14-3-3-ζKO mice (Figure 5F,G). Furthermore examination of genes associated with adipocyte maturity was performed, and significant reductions in adipocyte maturity genes, such as *Adipoq, Fabp4*, and *Retn*, could be detected in both iWAT and gWAT from adi14-3-3ζKO animals (Figure 5H,I). Despite the decreased levels of *Adipoq* mRNA in iWAT and gWAT, no differences in circulating adiponectin levels were observed, in addition to plasma leptin levels (Figure 5J,K).

The observed small, but significant impairments in *ex vivo* lipolysis (Figure 1H), decreases in the number of small (<200μm) adipocytes within gWAT (Figure 2D,F), and reductions in adipocyte maturity genes (Figure 5F,H), suggest the possibility that not all adipocytes within gWAT are affected by 14-3-3ζ deletion. Indeed, using immunohistochemistry, we confirmed the existence of a subset of adipocytes within gWAT that express 14-3-3ζ, and these adipocytes were undetectable in adi14-3-3ζKO mice (Figure 5L). Thus, the phenotype observed in adi14-3-3ζKO mice could be attributed to a specific subset of adipocytes within gWAT and that the loss of adipocyte maturity does not occur in all adipocytes within gWAT.

Depletion of 14-3-3ζ promotes adipocyte immaturity *in vitro*

To further characterize how reductions in 14-3-3ζ could affect adipocyte maturity, 3T3-L1 adipocytes were used. Initially, Oil Red-O incorporation was used as a surrogate measure of lipid content, and knockdown of 14-3-3ζ was found to significantly reduced lipids present in 3T3-L1 cells and was associated with marked

decreases in cells containing lipid droplets (Figure 6A,B). This was also confirmed by Bodipy 493/503 imaging and biochemical measurements of total TAGs, which were associated with significant decreases in the number of Bodipy-labelled lipid droplets and TAG content, respectively (Figure 6C,D). The impact of 14-3-3ζ depletion on TAG content was more pronounced in 3T3-L1 cells than in our *in vivo* model (Figure 6D vs Figure 5E), but this could be due to the heterogeneous expression of 14-3-3ζ within gWAT (Figure 5L). Similar to what was observed in adi14-3-3ζKO adipocytes, genes associated with *de novo* triglyceride synthesis and adipocyte maturity were significantly decreased (Figure 6E,F).

Knockdown of 14-3-3ζ is associated with distinct changes in the 3T3-L1 lipidome

During 3T3-L1 adipocyte differentiation, significant changes in the lipidome, including specific TAG species and sphingomyelins, have been observed [24]. In contrast, de-differentiation of primary, mature adipocytes is associated with changes in the abundance of specific lipid species [25]. Collectively, these findings suggest that the lipidomic signature of cells can be an alternative approach to assess adipocyte maturity. To this end, we used untargeted LC-MS lipidomics to interrogate lipid species that are changed upon depletion of 14-3-3ζ in mature 3T3-L1 cells and to confirm if loss of 14-3-3ζ generates lipidomic signature associated with adipocyte dedifferentiation (Figure 7A). A total of 2535 features were detected, of which 549 passed the selected stringent criteria of FDR<5% and FC >2 or < 0.5. A total of 139 annotated lipids from different lipid (sub)classes were significantly changed following 14-3-3ζ depletion (Figure 7B). For example, knockdown of 14-3-3ζ predominantly enriched monoacylglycerophosphocholines (LPC) and diacylglycerophosphocholines (PC), whereas diacylglycerophosphoethanolamines (PE and PE(O)) were reduced (Figure 7B, Table 1). The vast majority of altered lipid species (73/139) were triglycerides, and 14-3-3ζ depletion primarily decreased triglycerides species with lower acyl carbon chains and lower degrees of carbon bond saturation (Figure 7C).

It has been documented that following the differentiation of 3T3-L1 adipocytes, specific triglyceride species, like those with acyl carbon chain lengths ≥48 carbon lengths and those containing mono- and polyunsaturated species like TG 48:1, 48:2, and 48:3, are increased, whereas certain triglyceride species with 56 acyl carbon and 7 unsaturated bonds are decreased [24]. Of note, knockdown of 14-3-3ζ in mature 3T3-L1 adipocytes led to significant decreases in TG 48:n species and the converse enrichment of TG 56:n species, both of which are associated with a pre-adipocyte lipidome signature (Figure 7D; Table 1) [24]. When taken

together, these findings demonstrate that 14-3-3ζ depletion is promoting the acquisition of an immature phenotype.

Discussion

As 14-3-3ζ and its related isoforms are implicated in diverse metabolic processes, the primary aim of this study was to examine whether 14-3-3ζ had adipocyte-specific functions. This was to build on our prior studies that identified essential roles of 14-3-3ζ in adipogenesis [6, 9, 26-31]. We focused primarily on lipolysis, as the lipolytic enzymes ATGL and HSL are both phosphorylated by PKA to create 14-3-3 protein binding sites and found that reductions in 14-3-3ζ expression could attenuate lipolysis [16, 22]. Unexpectedly, we found that 14-3-3ζ was heterogeneously expressed in adipose tissue, which suggests that a subset of adipocytes depend on 14-3-3ζ for their physiological function, and that reducing 14-3-3ζ levels could decrease PPARγ2 expression and alter adipocyte maturity. Thus, the observed impairments in lipolysis due to reductions in 14-3-3ζ expression could be due to loss of adipocyte maturity and highlight novel roles of 14-3-3ζ in adipocyte biology and overall metabolism.

Through the use of adi14-3-3ζKO mice and 3T3-L1 cells, we demonstrate for the first time that 14-3-3ζ was necessary for lipolysis in primary adipocytes and expand our knowledge on the roles of 14-3-3 proteins in lipid metabolism, which was previously limited to fatty acid and lipid synthesis [29, 30, 32-34]. For example, 14-3-3 proteins have been shown to interact with ChREBP, a key transcription factor that regulates *de novo* lipogenesis, and prevent its translocation from the cytosol to the nucleus [32-34]. Our mechanistic studies to understand how 14-3-3ζ influences lipolysis first revealed that 14-3-3ζ-depletion in 3T3-L1 adipocytes impaired the lipolytic response to three agonists, namely isoproterenol, forskolin, and dbcAMP. Decreased HSL and CREB phosphorylation suggested that depletion of 14-3-3ζ impacted the kinase activity of PKA. Indeed, binding of 14-3-3 proteins to PKA has been shown to regulate PKA activity during growth cone turning responses in neurons, as binding of the RIIα and RIIβ regulatory subunits of PKA to 14-3-3 proteins modulate PKA activity [13].

Most striking was the observation that 14-3-3ζ could influence adipocyte maturity *in vitro* and *in vivo.* We found that reducing 14-3-3ζ expression in fully mature adipocytes significantly reduced PPARγ mRNA and protein levels and genes associated with mature adipocytes. This is in contrast to our previous work where we

described essential functions of 14-3-3ζ in adipogenesis, as siRNA-mediated depletion of 14-3-3ζ abrograted 3T3-L1 differentiation. Moreover, systemic deletion of 14-3-3ζ in mice significantly reduced adiposity and decreased gonadal fat mass and reduced the expression of mature adipocyte markers, such as PPARγ and FOXO1, within gWAT of systemic KO mice [6]. Thus, 14-3-3ζ represents a critical factor in both the differentiation of pre-adipocytes and maintenance of adipocyte identity and maturity. Adipocyte dedifferentiation has been documented in pregnancy, tissue repair, and tumorigenic transformations of liposarcomas [25, 35, 36], and dedifferentiation of visceral and subcutaneous human adipocytes, as noted by decreased mRNA expression of mature adipocyte gene markers including *PPARG2, C/EBPA, LPL,* and *ADIPOQ,* has been documented [37]. The cellular mechanisms underlying adipocyte dedifferentiation can be mediated by Notch receptor activation or canonical and non-canonical WNT signaling pathways [38-40]. For example, in 3T3-L1 cells, WNT3A-associated dedifferentiation occurs by increased levels of β-catenin, which results in the induction of specific genes leading to a loss of adipocyte identify [38]. As 14-3-3ζ has been shown to be a negative regulator of β-catenin localization and expression, reducing 14-3-3ζ abundance may promote dedifferentiation through a similar mechanism [41]. Further work is required to determine whether immature 14-3-3ζ-expressing adipocytes can be transdifferentiated into other cell types, as dedifferentiated adipocytes can display multipotency and can transdifferentiated into macrophages, endothelial cells, or osteoblasts [38, 42-44].

In addition to affecting adipocyte maturity, depletion of 14-3-3ζ was also associated with marked decreases in triglyceride content and genes associated with lipid synthesis. In differentiating 3T3-L1 cells, distinct changes in the lipidome signature have been reported, whereby certain lipid species, such as triglycerides of varying acyl carbon lengths, are increased or decreased during differentiation [24]. Our unbiased lipidomic analysis revealed over 139 unique lipid species, predominantly triglycerides, whose abundance were significantly changed following 14-3-3ζ knockdown. Reducing 14-3-3ζ expression decreased levels of triglyceride species with shorter chain ≤ 54 and low number of unsaturations associated with fully differentiated 3T3-L1 cells and increased species with longer chain >54 and high number of unsaturation of undifferentiated cells [24]. The exact mechanism by which 14-3-3ζ knockdown in 3T3-L1 cells reduces intracellular lipids is not known, but it is possible that autophagy, which we have previously shown to be up-regulated by 14-3-3ζ depletion, could be a potential contributor [6, 45]. Alternatively, dedifferentiation of adipocytes is also associated with a rapid secretion of lipid droplets via a yet unknown mechanism [46].

Within a given adipose depot, it is now appreciated that heterogeneous populations of adipocytes are present. These adipocytes arise from different progenitors pools, such as those expressing DPP4, WT1, and PDFRα [47-51]. In the present study, we found that 14-3-3ζ is heterogeneously expressed in within a sub-set of adipocytes within gWAT of male mice, and the loss of 14-3-3ζ in these cells may account for the small, but significant, reductions in the expression of adipocyte maturity, lipolytic, and lipogenic genes in gWAT. To further characterize these cells, appropriate lineage tracing or reporter mice are clearly needed, and given that adipocytes within each depot may have different metabolic phenotypes [48], such tools would be critical to further define their metabolic contributions.

While the initial intent of this study was to understand the contribution of 14-3-3ζ to lipolysis, additional experiments are required to fully understand whether 14-3-3ζ regulates other aspects of adipocyte function. We previously reported that systemic 14-3-3ζ knockout mice displayed reduced adiposity, whereas transgenic mice overexpressing 14-3-3ζ gained more weight on a high-fat diet, suggesting that 14-3-3ζ promotes adipose tissue expansion [6]. Thus, placement of adi14-3-3ζKO mice on a high-fat diet will aid in assessing whether 14-3-3ζ is necessary for the development of diet-induced obesity. Decreased PPARγ expression in mouse adipocytes impairs WAT and BAT formation, as well as diet-induced obesity [52, 53], and given that adipocyte-specific deletion of 14-3-3ζ reduced PPARγ2 levels in gWAT (Figure 5D), deletion of 14-3-3ζ may also confer protection to diet-induced obesity. The regulatory roles of 14-3-3 proteins on AS160/TBC1D4 have been well-documented *in vitro* and *in vivo* [9, 54], and we initially hypothesized that deletion of 14-3-3ζ in adipocytes would result in adipocyte-specific impairments in GLUT4 translocation. However, in contrast to our previous studies with systemic 14-3-3ζ knockout mice where we detected decreased insulin sensitivity [6], no differences were observed in adi14-3-3ζKO mice. Thus, these findings suggest that the decrease in insulin sensitivity in systemic 14-3-3ζKO mice could be specific to skeletal muscle, which is the primary site of glucose disposal [55].

Collectively, results from our *in vivo* and *in vitro* models demonstrate that decreased 14-3-3ζ expression influences lipolysis via alterations in adipocyte maturity. To date, the roles of 14-3-3ζ in adipocytes are not fully known, and when taken with our previous work, this study highlights the complex functions of 14-3-3ζ in adipocytes. Additional studies are needed to further characterize the differences between adipocytes that do and do not express 14-3-3ζ, and increasing our understanding how 14-3-3ζ may regulate adipocyte function may lead to the development of novel approaches to treat lipid abnormalities stemming from obesity.

Acknowledgments

The authors would like to thank Mina Sadeghi and Dr. Yves Mugabo for their technical assistance with various experiments. The authors would also like to thank the CRCHUM Histological core and the Transgenesis and Animal Modeling Core for assistance with histology and the rederivation of *Ywhaz*$^{flox/flox}$ mice, respectively. This work was supported by a CIHR Project (PJT-153144) grant to GEL and benefited from an infrastructure grant supported by the Canadian Foundation for Innovation and by the Montreal Heart Foundation to CDR. GEL holds the Canada Research Chair in Adipocyte Development, and AO was supported by a CIHR Canada Graduate Scholarship- Master's (CGS-M) award.

Authors contributions:

A.O. designed the studies, carried out the research, interpreted the results, and wrote the manuscript. K.D. performed experiments and edited the manuscript. IRF performed experiments and analyzed data. C.D. contributed to study design and edited the manuscript. G.E.L. conceived the concept, designed and performed studies, interpreted the results, and wrote and revised the manuscript. G.E.L is the guarantor of this work.

Disclosure statement: The authors have nothing to disclose.

Figure legends

Figure 1- Deletion of 14-3-3ζ in adipocytes impairs lipolysis. (A) Experimental design to examine the role of 14-3-3ζ in lipolysis. *Adipoq*-CreERT2^{Soff} mice were bred with those harboring Loxp sites flanking exon4 of *Ywhaz*, the gene encoding 14-3-3ζ. At 8-weeks of age, wildtype (WT) or adi14-3-3ζKO (KO) mice were injected with tamoxifen (TMX, 50 mg/kg; 5 days), and mice were use for experimental procedures 4 weeks after the last TMX injection. **(B)** Levels of *Ywhaz, Ywhab, Ywhag, Ywhae, Ywhah, Ywhas* and *Ywhaq* (encoding 14-3-3ζ, 14-3-3β, 14-3-3γ, 14-3-3ε, 14-3-3η, 14-3-3σ, and 14-3-3θ, respectively) in gonadal (gWAT) and inguinal (iWAT) adipose depots of male WT or adi14-3-3ζKO mice (n=8-9 WT, n=5 KO for male mice, *: $p<0.05$ when compared

to WT). **(C)** Body weights of male adi14-3-3ζKO mice following i.p injections of tamoxifen (50 mg/kg b.w) were measured weekly (n=9 WT, n=6 KO for male mice). **(D,E)** Intraperitoneal glucose (2 g/kg b.w.) (D) and insulin (0.5 U/kg b.w.) (E) tolerance tests on male adi14-3-3ζKO mice fasted for 6 and 4 hours, respectively, at 12 weeks of age (n=9 WT, n=6 KO for male mice). **(F)** Plasma insulin levels from WT and adi14-3-3ζKO mice following an overnight fast (n=9 WT, n=6 KO**). (G)** Plasma glycerol and FFA levels in male adi14-3-3ζKO mice after injection with CL-316,243 (CL, 1 mg/kg b.w.), following an overnight fast (n=9 WT, n=6 KO; *: p<0.05 when compared to -CL, #: p<0.05 when compared to WT). **(H)** Glycerol and FFA levels in the supernatant of gonadal adipose tissue explants treated with isoproterenol (Iso, 1 μM) for 2 hours. Glycerol and FFA release were normalized to the mass of the explants (n=5 WT, n=3 KO; #: p<0.05 when compared to WT).

Figure 2- Loss of 14-3-3ζ in gonadal white adipocytes affects adipocyte size. (A-F) Immunofluorescent staining was used to examine adipocyte morphology (A, D), average size (B,E), and distrubtion (C,F) in inguinal white adipose tissue (iWAT, A-C) or gonadal white adipose tissue (gWAT, D-F) of male WT and KO mice. (Representative images of n=4 mice per group; scale bar= 200 μm).

Figure 3- Depletion of 14-3-3ζ in mature 3T3-L1 adipocytes impairs lipolysis in response to mulitple stimuli. (A,B) Depletion of 14-3-3ζ with siRNA in mature 3T3-L1 adipocytes was confirmed by qPCR (A) (n=6; *= p<0.05 vs. siCon) and immunoblotting of cell lysates for 14-3-3ζ (B) (n=3 per condition). **(C)** Levels of *Ywhab, Ywhag, Ywhae, Ywhah, Ywhas* and *Ywhaq* (encoding 14-3-3β, 14-3-3γ, 14-3-3ε, 14-3-3η, 14-3-3σ, and 14-3-3θ, respectively) mRNA were measured in 14-3-3ζ-depleted 3T3-L1 adipocytes (n=6 per group). **(D)** Levels of glycerol (C) and FFA (D) released by siRNA-transfected 3T3-L1 adipocytes treated with isoproterenol (Iso, 1 μM), forskolin (10 μM) with IMBX (0.5 mM), or dibutyryl cAMP (dbcAMP, 1 mM) for 2 hours (n=6 per condition; *= p<0.05 when compared to respective treatment in siCon-transfected cells).

Figure 4- 14-3-3ζ is required for the expression of lipolytic effectors. (A,B) Quantitative PCR was used to measure mRNA levels of β-adrenergic receptor (A) and phosphodiesterase (B) isoforms in 14-3-3ζ-depleted 3T3-L1 adipocytes (n=6 per group; *= p<0.05 when compared to siCon). **(C)** Intracellular cAMP levels of siRNA-transfected 3T3-L1 lysates treated with isoproterenol (ISO, 1 μM) or forskolin (20 μM) for 1 hour (n=6-7 per group). **(D)** mRNA levels of *Atgl* and *Hsl* in mature 3T3-L1 cells following siRNA-mediated knockdown of 14-3-3ζ

(n=6 per group; *= p<0.05 when compared to siCon). **(E)** Immunoblotting for phosphorylated and total forms of HSL and CREB in siRNA-transfected 3T3-L1 lysates treated with isoproterenol (ISO, 1 μM), forskolin (10 μM) with IMBX (0.5 mM), or dbCAMP (1 mM) (n=6 per group).

Figure 5- Adipocyte-specific deletion of 14-3-3ζ decreases expression of genes associated with adipocyte maturity *in vivo*. (A,B) Quantitative PCR was used to measure mRNA levels of *Atgl* and *Hsl* (A) and *Pparg* (B) in gonadal (gWAT) and inguinal (iWAT) adipose tissues of male adi14-3-3ζKO mice (n=6 per genotype). **(C-D)** Immunoblotting was used to measure total levels of ATGL (C) and HSL and PPARγ (D) in gWAT of male adi14-3-3ζKO mice (representative of n=6 per genotype). **(E)** Total triacylglycerols (TAGs) were measured in gWAT and iWAT of WT and adi14-3-3ζKO (KO) mice. Data were normalized to total protein of each sample (n=6 per genotype). **(F-I)** Genes associated with *de novo* triglyceride synthesis (F,G) and adipocyte maturity (H,I) were measured in gWAT (F,H) and iWAT (G,I) of WT or adi14-3-3ζKO mice (n=6 per genotype, *: p<0.05 when compared to WT mice). **(J,K)** Leptin (J) and adiponectin (K) levels were determined from WT and adi14-3-3ζKO mouse plasma collected after an over-night fast (n=6 per genotype). **(L)** Immunohistochemistry was performed on paraffin-embedded gWAT sections of WT and adi14-3-3ζKO mice. Arrowheads denote adipocytes that display 14-3-3ζ immunoreactivity. (representative images of n=4 mice per group).

Figure 6- Knockdown of 14-3-3ζ by siRNA promotes dedifferentiation *in vitro*. (A) Oil Red-O incorporation was used to assess triglyceride levels in siCon- and si14-3-3ζ-transfected mature 3T3-L1 adipocytes (n=4; *= p<0.05 siCon vs si14-3-3ζ). **(B)** Visualization of Oil Red-O incorporated control (siCon) and 14-3-3ζ-depleted (si14-3-3ζ) 3T3-L1 adipocytes by light microscopy (representative images of n=4 per treatment). **(C)** Lipid droplets were visualized by immunofluorescent imaging of incorporated Bodipy 493/504. Hoechst 33342 was used to visualize nuclei (representative image of transfected cells, scale bar= 25 μm). **(D)** Total triglycerides were measured in mature 3T3-L1 adipocytes transfected with a scrambled control (siCon) or siRNA against 14-3-3ζ (si14-3-3ζ) (n=6; *= p<0.05 siCon vs si14-3-3ζ). **(E,F)** Following transfection with siRNA against 14-3-3ζ (si14-3-3ζ) or a scrambled control (siCon), mRNA was isolated, followed by quantitative PCR for genes

associated with *de novo* triglyceride synthesis (E) or adipocyte maturity (F) (n=6 per group, *: p<0.05 when compared to siCon).

Figure 7- Distinct changes in the lipidome of mature 3T3-L1 cells following 14-3-3ζ knockdown.

(A) Fully differentiated 3T3-L1 were electroporated with control siRNA (siCon) or siRNA against 14-3-3ζ (si14-3-3ζ), and after 48 hours, cells were collected in methanol for lipid extraction and subsequent untargeted LC-MS lipidomics. **(B)** Volcano plot depicting the 2425 features obtained following data processing. The *x* axis corresponds to fold changes (FCs) of MS signal intensity values for all these features in siCon vs si14-3-3ζ cells (in log2) and the *y* axis to *P* values (–log10). Using the selected threshold (corrected *P*-value<0.05 corresponding to a FDR<5% and FC<2 or <0,5), 549 features were found to significantly discriminate siCon vs si14-3-3ζ cells, of which 139 unique lipids from various (sub)classes (shown using color symbols) were identified using an in-house reference database. The in-set table list the number of lipid species that were found to be up- or down-regulated according to the different lipid (sub)classes following 14-3-3ζ depletion. **(C)** Triglycerides that were significantly up- or down-regulated after 14-3-3ζ knockdown were categorized by acyl carbon chain length or by the degree of saturation. **(D)** Triglycerides species that are normally enriched (TG 48:n) or depleted (TG 56:n) in differentiated 3T3-L1 cells (gray columns) were found to be significantly affected by 14-3-3ζ depletion (n=5 per group).

Supplemental Figure legends

Figure S1- Deletion of 14-3-3ζ in adipose tissue of female mice does promote metabolic dysfunction.

(A) Levels of *Ywhaz* mRNA were measured by quantitative PCR in gonadal (gWAT) and inguinal (iWAT) adipose tissue from female adi14-3-3ζKO mice (n=8 per genotype). **(B)** Body weights of female adi14-3-3ζKO mice following i.p injections of tamoxifen (50 mg/kg b.w) were measured weekly (n=8 per genotype). **(C,D)** Intraperitoneal glucose (2 g/kg b.w.) (D) and insulin (0.5 U/kg b.w.) (E) tolerance tests on female adi14-3-3ζKO mice fasted for 6 and 4 hours, respectively, at 12 weeks of age (n=8 per genotype). **(E,F)** Plasma glycerol and FFA levels in female adi14-3-3ζKO (E) and TAP (F) mice after injection with CL-316,243 (CL, 1 mg/kg b.w.) or isoproterenol (ISO, 1 mg/kg b.w.) following an overnight fast (adi14-3-3ζKO: n=8 WT, n=8 KO; TAP: n=9 WT, n=12 TAP).

Figure S2- Over-expression of 14-3-3ζ does not affect lipolysis in male mice. (A) After an over-night fast, body weights from male wild-type (WT) and TAP-14-3-3ζ over-expressing transgenic mice (TAP) were obtained (n=6 WT, n=9 TAP mice). **(B)** Following an overnight fast, plasma glycerol and FFA levels in male wild-type (WT) and TAP-14-3-3ζ over-expressing transgenic mice (TAP) were measured after an intraperitoneal injection with isoproterenol (ISO; 10 mg/kg b.w.) (n=6 WT, n=9 TAP mice). **(C)** Mature 3T3-L1 adipocytes were transfected with plasmids containing GFP (2 μg) or 14-3-3ζ IRES-GFP (2 μg), and over-expression was confirmed by immunoblotting (n=4 per group). **(D)** Free fatty acid (FFA) release into the supernatant after a 2-hour incubation with isoproterenol (ISO, 1 μM.) was measured from GFP or 14-3-3ζ IRES-GFP 3T3-L1 adipocytes (n=4, *: $p<0.05$ when comparing ISO treatments).

References

1. Duncan, R.E., et al., *Regulation of lipolysis in adipocytes.* Annu Rev Nutr, 2007. **27**: p. 79-101.
2. Anthonsen, M.W., et al., *Identification of novel phosphorylation sites in hormone-sensitive lipase that are phosphorylated in response to isoproterenol and govern activation properties in vitro.* J Biol Chem, 1998. **273**(1): p. 215-21.
3. Holm, C., *Molecular mechanisms regulating hormone-sensitive lipase and lipolysis.* Biochem Soc Trans, 2003. **31**(Pt 6): p. 1120-4.
4. Ferl, R.J., M.S. Manak, and M.F. Reyes, *The 14-3-3s.* Genome Biol, 2002. **3**(7): p. Reviews3010.
5. Mhawech, P., *14-3-3 proteins--an update.* Cell Res, 2005. **15**(4): p. 228-36.
6. Lim, G.E., et al., *14-3-3zeta coordinates adipogenesis of visceral fat.* Nat Commun, 2015. **6**: p. 7671.
7. Fu, H., R.R. Subramanian, and S.C. Masters, *14-3-3 proteins: structure, function, and regulation.* Annu Rev Pharmacol Toxicol, 2000. **40**: p. 617-47.
8. Dougherty, M.K. and D.K. Morrison, *Unlocking the code of 14-3-3.* J Cell Sci, 2004. **117**(Pt 10): p. 1875-84.
9. Ramm, G., et al., *A role for 14-3-3 in insulin-stimulated GLUT4 translocation through its interaction with the RabGAP AS160.* J Biol Chem, 2006. **281**(39): p. 29174-80.
10. Brunet, A., et al., *14-3-3 transits to the nucleus and participates in dynamic nucleocytoplasmic transport.* J Cell Biol, 2002. **156**(5): p. 817-28.
11. Mugabo, Y., et al., *Elucidation of the 14-3-3zeta interactome reveals critical roles of RNA-splicing factors during adipogenesis.* J Biol Chem, 2018. **293**(18): p. 6736-6750.
12. Kleppe, R., et al., *The 14-3-3 proteins in regulation of cellular metabolism.* Semin Cell Dev Biol, 2011. **22**(7): p. 713-9.
13. Kent, C.B., et al., *14-3-3 proteins regulate protein kinase a activity to modulate growth cone turning responses.* J Neurosci, 2010. **30**(42): p. 14059-67.
14. Fantl, W.J., et al., *Activation of Raf-1 by 14-3-3 proteins.* Nature, 1994. **371**(6498): p. 612-4.
15. Kim, D., et al., *Regulation of Dyrk1A kinase activity by 14-3-3.* Biochem Biophys Res Commun, 2004. **323**(2): p. 499-504.
16. Marvyn, P.M., et al., *Fasting upregulates adipose triglyceride lipase and hormone-sensitive lipase levels and phosphorylation in mouse kidney.* Biochem Cell Biol, 2015. **93**(3): p. 262-7.
17. Dickinson, M.E., et al., *High-throughput discovery of novel developmental phenotypes.* Nature, 2016. **537**(7621): p. 508-514.
18. Angrand, P.O., et al., *Transgenic mouse proteomics identifies new 14-3-3-associated proteins involved in cytoskeletal rearrangements and cell signaling.* Mol Cell Proteomics, 2006. **5**(12): p. 2211-27.
19. Lim, G.E., et al., *Ywhaz/14-3-3zeta Deletion Improves Glucose Tolerance Through a GLP-1-Dependent Mechanism.* Endocrinology, 2016. **157**(7): p. 2649-59.
20. McQuin, C., et al., *CellProfiler 3.0: Next-generation image processing for biology.* PLoS Biol, 2018. **16**(7): p. e2005970.
21. Forest, A., et al., *Comprehensive and Reproducible Untargeted Lipidomic Workflow Using LC-QTOF Validated for Human Plasma Analysis.* J Proteome Res, 2018. **17**(11): p. 3657-3670.
22. Ahmadian, M., et al., *Desnutrin/ATGL is regulated by AMPK and is required for a brown adipose phenotype.* Cell Metab, 2011. **13**(6): p. 739-48.
23. Takenaka, A., et al., *Human-specific SNP in obesity genes, adrenergic receptor beta2 (ADRB2), Beta3 (ADRB3), and PPAR gamma2 (PPARG), during primate evolution.* PLoS One, 2012. **7**(8): p. e43461.
24. Liaw, L., et al., *Lipid Profiling of In Vitro Cell Models of Adipogenic Differentiation: Relationships With Mouse Adipose Tissues.* J Cell Biochem, 2016. **117**(9): p. 2182-93.
25. Bi, P., et al., *Notch activation drives adipocyte dedifferentiation and tumorigenic transformation in mice.* J Exp Med, 2016. **213**(10): p. 2019-37.
26. Bunney, T.D., H.S. van Walraven, and A.H. de Boer, *14-3-3 protein is a regulator of the mitochondrial and chloroplast ATP synthase.* Proc Natl Acad Sci U S A, 2001. **98**(7): p. 4249-54.
27. Bustos, D.M. and A.A. Iglesias, *A model for the interaction between plant GAPN and 14-3-3zeta using protein-protein docking calculations, electrostatic potentials and kinetics.* J Mol Graph Model, 2005. **23**(6): p. 490-502.
28. Danial, N.N., et al., *Dual role of proapoptotic BAD in insulin secretion and beta cell survival.* Nat Med, 2008. **14**(2): p. 144-53.
29. Meek, S.E., W.S. Lane, and H. Piwnica-Worms, *Comprehensive proteomic analysis of interphase and mitotic 14-3-3-binding proteins.* J Biol Chem, 2004. **279**(31): p. 32046-54.

30. Pozuelo Rubio, M., et al., *14-3-3-affinity purification of over 200 human phosphoproteins reveals new links to regulation of cellular metabolism, proliferation and trafficking.* Biochem J, 2004. **379**(Pt 2): p. 395-408.
31. Pozuelo Rubio, M., et al., *14-3-3s regulate fructose-2,6-bisphosphate levels by binding to PKB-phosphorylated cardiac fructose-2,6-bisphosphate kinase/phosphatase.* Embo j, 2003. **22**(14): p. 3514-23.
32. Ge, Q., et al., *Structural characterization of a unique interface between carbohydrate response element-binding protein (ChREBP) and 14-3-3beta protein.* J Biol Chem, 2012. **287**(50): p. 41914-21.
33. Horton, J.D., J.L. Goldstein, and M.S. Brown, *SREBPs: activators of the complete program of cholesterol and fatty acid synthesis in the liver.* J Clin Invest, 2002. **109**(9): p. 1125-31.
34. Sakiyama, H., et al., *Regulation of nuclear import/export of carbohydrate response element-binding protein (ChREBP): interaction of an alpha-helix of ChREBP with the 14-3-3 proteins and regulation by phosphorylation.* J Biol Chem, 2008. **283**(36): p. 24899-908.
35. Corsa, C.A.S. and O.A. MacDougald, *Cyclical Dedifferentiation and Redifferentiation of Mammary Adipocytes.* Cell Metab, 2018. **28**(2): p. 187-189.
36. Liao, Y., et al., *In vivo dedifferentiation of adult adipose cells.* PLoS One, 2015. **10**(4): p. e0125254.
37. Matsumoto, T., et al., *Mature adipocyte-derived dedifferentiated fat cells exhibit multilineage potential.* J Cell Physiol, 2008. **215**(1): p. 210-22.
38. Gustafson, B. and U. Smith, *Activation of canonical wingless-type MMTV integration site family (Wnt) signaling in mature adipocytes increases beta-catenin levels and leads to cell dedifferentiation and insulin resistance.* The Journal of biological chemistry, 2010. **285**(18): p. 14031-14041.
39. Bi, P., et al., *Notch activation drives adipocyte dedifferentiation and tumorigenic transformation in mice.* The Journal of experimental medicine, 2016. **213**(10): p. 2019-2037.
40. Zoico, E., et al., *Adipocytes WNT5a mediated dedifferentiation: a possible target in pancreatic cancer microenvironment.* Oncotarget, 2016. **7**(15): p. 20223-35.
41. Li, F.-Q., et al., *Chibby cooperates with 14-3-3 to regulate beta-catenin subcellular distribution and signaling activity.* The Journal of cell biology, 2008. **181**(7): p. 1141-1154.
42. Soejima, K., et al., *Effects of mature adipocyte-derived dedifferentiated fat (DFAT) cells on generation and vascularisation of dermis-like tissue after artificial dermis grafting.* Journal of plastic surgery and hand surgery, 2015. **49**(1): p. 25-31.
43. Kishimoto, N., et al., *Dedifferentiated fat cells differentiate into osteoblasts in titanium fiber mesh.* Cytotechnology, 2013. **65**(1): p. 15-22.
44. Sparks, R.L., et al., *Differentiation, dedifferentiation, and transdifferentiation of BALB/c 3T3 T mesenchymal stem cells: potential significance in metaplasia and neoplasia.* Cancer research, 1986. **46**(10): p. 5312-5319.
45. Dong, H. and M.J. Czaja, *Regulation of lipid droplets by autophagy.* Trends in endocrinology and metabolism: TEM, 2011. **22**(6): p. 234-240.
46. Côté, J.A., et al., *Characterization and visualization of the liposecretion process taking place during ceiling culture of human mature adipocytes.* Journal of cellular physiology, 2019. **234**(7): p. 10270-10280.
47. Jiang, Y., et al., *Independent stem cell lineages regulate adipose organogenesis and adipose homeostasis.* Cell reports, 2014. **9**(3): p. 1007-1022.
48. Lee, K.Y., et al., *Developmental and functional heterogeneity of white adipocytes within a single fat depot.* EMBO J, 2019. **38**(3).
49. Merrick, D., et al., *Identification of a mesenchymal progenitor cell hierarchy in adipose tissue.* Science, 2019. **364**(6438).
50. Sanchez-Gurmaches, J. and D.A. Guertin, *Adipocytes arise from multiple lineages that are heterogeneously and dynamically distributed.* Nat Commun, 2014. **5**: p. 4099.
51. Vishvanath, L., et al., *Pdgfrβ+ Mural Preadipocytes Contribute to Adipocyte Hyperplasia Induced by High-Fat-Diet Feeding and Prolonged Cold Exposure in Adult Mice.* Cell metabolism, 2016. **23**(2): p. 350-359.
52. Koutnikova, H., et al., *Compensation by the muscle limits the metabolic consequences of lipodystrophy in PPAR gamma hypomorphic mice.* Proc Natl Acad Sci U S A, 2003. **100**(24): p. 14457-62.
53. Wang, F., et al., *Lipoatrophy and severe metabolic disturbance in mice with fat-specific deletion of PPARgamma.* Proc Natl Acad Sci U S A, 2013. **110**(46): p. 18656-61.
54. Chen, S., et al., *Mice with AS160/TBC1D4-Thr649Ala knockin mutation are glucose intolerant with reduced insulin sensitivity and altered GLUT4 trafficking.* Cell Metab, 2011. **13**(1): p. 68-79.

55. DeFronzo, R.A. and D. Tripathy, *Skeletal muscle insulin resistance is the primary defect in type 2 diabetes.* Diabetes Care, 2009. **32 Suppl 2**: p. S157-63.

Table 1- List of lipid species that were significantly up- and down-regulated following 14-3-3ζ depletion

Lipids selection
Normalisation cyclioess;
Unpaired t-test
With Benjamini-Hochberg correction
FDR<5%
FC>2
549 significatively different entities from which:
86 unique lipids annotated with Metlin and confirmed by manual inspection
53 unique lipids identified with their acyl-chains using our in-house database

Down regulated entities

Compound	ionisation mode	Masse	m/z	RT	Adduct	p	p (Corr)	FC (abs)	Regulation (SiZeta vs SiCon)	FC
LPC24:0	POS	607.4558	608.4636	16.71	[M+H]+	1.22E-03	5.22E-03	2.66	down	-2.66
PE(14:0_22:6)	POS	735.4838	736.4916	17.99	[M+H]+	5.86E-04	3.08E-03	2.12	down	-2.12
PE(16:0_18:1)	POS	717.5301	718.5379	26.12	[M+H]+	8.47E-06	1.83E-04	2.05	down	-2.05
PE(34:2)	POS	715.5146	716.5224	22.86	[M+H]+	4.66E-06	1.17E-04	2.95	down	-2.95
PE(36:2)	POS	743.5465	744.5543	26.52	[M+H]+	1.28E-05	2.38E-04	2.27	down	-2.27
PE(O-18:0/18:1)	POS	731.5832	732.591	32.48	[M+H]+	1.67E-04	1.33E-03	3.12	down	-3.12
PE(O-18:1/18:1)	POS	729.5661	730.5739	31.82	[M+H]+	1.38E-03	5.72E-03	3.71	down	-3.71
PE(O-18:2/18:2)	POS	725.5349	726.5427	25.52	[M+H]+	5.78E-05	6.54E-04	8.72	down	-8.72
PE(O-36:3)	POS	727.551	728.5588	28.82	[M+H]+	1.03E-04	9.63E-04	3.35	down	-3.35
PE(O-34:3)	POS	699.5192	700.527	24.95	[M+H]+	4.85E-05	5.90E-04	3.89	down	-3.89
PE(O-34:2)	POS	701.5323	702.5401	27.78	[M+H]+	1.13E-04	1.02E-03	3.99	down	-3.99
PI(16:0_20:4)	POS	875.5525	876.5603	18.17	[M+NH4]+	9.78E-06	2.01E-04	2.21	down	-2.21
TG(16:0_15:0_18:1)	POS	840.722	841.7298	55.85	[M+Na]+	1.45E-04	1.22E-03	2.14	down	-2.14
TG(16:0_16:0_18:1)	POS	854.7393	855.7471	59.61	[M+Na]+	1.96E-04	1.47E-03	2.37	down	-2.37
TG(18:2_18:2_12:0)	POS	815.7022	816.71	42.55	[M+NH4]+	5.45E-05	6.25E-04	3.37	down	-3.37
TG(18:3_181_12:0)	POS	815.7027	816.7105	42.79	[M+NH4]+	1.35E-04	1.15E-03	2.13	down	-2.13
TG 39:0	POS	697.6248	698.6326	40.4	[M+NH4]+	1.80E-06	6.32E-05	2.98	down	-2.98
TG 39:0	POS	697.6248	698.6326	40	[M+NH4]+	1.91E-04	1.44E-03	2.11	down	-2.11
TG 39:1	POS	695.6087	696.6165	38.62	[M+NH4]+	4.76E-05	5.88E-04	4.14	down	-4.14
TG 40:1	POS	709.6248	710.6326	39.55	[M+NH4]+	7.19E-06	1.66E-04	3.26	down	-3.26
TG 40:2	POS	707.6085	708.6163	37.94	[M+NH4]+	3.30E-05	4.59E-04	3.54	down	-3.54
TG 41:0	POS	725.6559	726.6637	42.74	[M+NH4]+	1.11E-07	9.60E-06	2.64	down	-2.64
TG 41:1	POS	723.6399	724.6477	40.56	[M+NH4]+	4.65E-06	1.17E-04	3.58	down	-3.58
TG 41:2	POS	721.6242	722.632	38.8	[M+NH4]+	2.38E-05	3.60E-04	4.03	down	-4.03
TG 42:2	POS	735.6393	736.6471	39.72	[M+NH4]+	1.24E-05	2.38E-04	3.69	down	-3.69
TG 43:0	POS	753.6882	754.696	45.99	[M+NH4]+	1.22E-05	2.38E-04	2.17	down	-2.17
TG 43:1	POS	751.671	752.6788	42.51	[M+NH4]+	6.52E-04	3.29E-03	3.08	down	-3.08
TG 43:1	POS	751.6709	752.6787	42.95	[M+NH4]+	2.17E-05	3.48E-04	2.87	down	-2.87
TG 43:2	POS	749.6569	750.6647	41.14	[M+NH4]+	3.18E-03	1.06E-02	3.29	down	-3.29
TG 43:2	POS	749.6555	750.6633	40.7	[M+NH4]+	7.98E-06	1.80E-04	3.21	down	-3.21
TG 43:3	POS	747.6403	748.6481	39.08	[M+NH4]+	2.18E-05	3.48E-04	3.55	down	-3.55
TG 44:1	POS	765.6875	766.6953	45.28	[M+NH4]+	2.44E-04	1.69E-03	17.67	down	-17.67
TG 44:1	POS	765.6871	766.6949	43.96	[M+NH4]+	9.51E-04	4.28E-03	7.54	down	-7.54
TG 44:2	POS	763.6717	764.6795	42.39	[M+NH4]+	7.08E-04	3.48E-03	3.14	down	-3.14
TG 44:2	POS	763.6706	764.6784	41.86	[M+NH4]+	6.05E-05	6.62E-04	2.55	down	-2.55
TG 44:3	POS	761.6561	762.6639	40.25	[M+NH4]+	5.36E-05	6.25E-04	3.25	down	-3.25
TG 44:3	POS	761.6557	762.6635	39.94	[M+NH4]+	1.57E-04	1.29E-03	3.07	down	-3.07
TG 45:1	POS	779.7032	780.711	45.64	[M+NH4]+	1.26E-04	1.09E-03	4.46	down	-4.46
TG 45:2	POS	777.6873	778.6951	43.79	[M+NH4]+	1.22E-03	5.22E-03	2.64	down	-2.64
TG 45:3	POS	775.6706	776.6784	40.93	[M+NH4]+	4.04E-04	2.44E-03	2.47	down	-2.47
TG 45:4	POS	773.6569	774.6647	39.49	[M+NH4]+	1.04E-02	2.71E-02	2.97	down	-2.97
TG 46:1	POS	793.7186	794.7264	47.63	[M+NH4]+	4.13E-04	2.46E-03	2.09	down	-2.09
TG 46:3	POS	789.6866	790.6944	42.56	[M+NH4]+	2.42E-03	8.54E-03	2.35	down	-2.35
TG 46:4	POS	787.6688	788.6766	40.44	[M+NH4]+	6.79E-05	7.14E-04	3.65	down	-3.65
TG 46:4	POS	787.6686	788.6764	40.98	[M+NH4]+	3.68E-03	1.19E-02	2.77	down	-2.77
TG 47:1	POS	807.7336	808.7414	51.35	[M+NH4]+	7.30E-04	3.56E-03	2.01	down	-2.01
TG 47:2	POS	805.7191	806.7269	45.9	[M+NH4]+	2.11E-03	7.74E-03	2.70	down	-2.70
TG 47:3	POS	803.7031	804.7109	44.01	[M+NH4]+	1.54E-03	6.18E-03	2.41	down	-2.41
TG 47:4	POS	801.6871	802.6949	41.54	[M+NH4]+	7.89E-05	7.99E-04	3.21	down	-3.21
TG 48:3	POS	817.7181	818.7259	45.7	[M+NH4]+	6.81E-03	1.95E-02	2.68	down	-2.68
TG 49:3	POS	831.7349	832.7427	47.66	[M+NH4]+	1.72E-03	6.64E-03	3.87	down	-3.87
TG 49:3	POS	859.7577	860.7655	49.06	[M+NH4]+	1.02E-02	2.67E-02	2.11	down	-2.11
TG 49:4	POS	829.7197	830.7275	44.25	[M+NH4]+	1.33E-05	2.47E-04	2.99	down	-2.99
TG 49:4	POS	829.7191	830.7269	45.08	[M+NH4]+	9.04E-04	4.16E-03	2.98	down	-2.98
TG 49:4	POS	829.719	830.7268	44.6	[M+NH4]+	1.10E-04	1.00E-03	2.81	down	-2.81
TG 49:4	POS	829.7197	830.7275	43.91	[M+NH4]+	6.31E-05	6.70E-04	2.75	down	-2.75
TG 49:5	POS	827.7039	828.7117	42	[M+NH4]+	7.08E-04	3.48E-03	4.50	down	-4.50
TG 50:4	POS	843.7345	844.7423	45.96	[M+NH4]+	2.17E-05	3.48E-04	2.38	down	-2.38
TG 50:4	POS	843.734	844.7418	46.92	[M+NH4]+	1.10E-03	4.86E-03	2.14	down	-2.14
TG 50:5	POS	841.7172	842.725	43.32	[M+NH4]+	2.49E-05	3.74E-04	4.04	down	-4.04
TG 51:5	POS	855.735	856.7428	44.86	[M+NH4]+	4.58E-04	2.64E-03	4.46	down	-4.46
TG 51:5	POS	855.7338	856.7416	45.32	[M+NH4]+	2.67E-04	1.82E-03	2.76	down	-2.76
TG 53:4	POS	885.777	886.7848	47.44	[M+NH4]+	8.33E-03	2.27E-02	2.46	down	-2.46
TG 53:5	POS	883.7652	884.773	48.15	[M+NH4]+	3.14E-04	2.05E-03	2.20	down	-2.20

UP regulated

Compound	ionisation r	Masse	m/z	RT	Adduct	p	p (Corr)	FC (abs)	Regulation (Si	Zeta FC
LPC14:0-a	POS	467.2995	468.3073	6.7	[M+H]+	2.77E-03	9.54E-03	3.82	Up	3.82
LPC15:0	POS	481.3152	482.323	7.92	[M+H]+	1.58E-02	3.82E-02	2.06	Up	2.06
LPC18:1 bc	POS	521.3474	522.3552	9.49	[M+H]+	8.11E-03	2.22E-02	2.25	Up	2.25
LPC19:0-b	POS	537.3784	538.3862	11.59	[M+H]+	2.68E-06	8.10E-05	2.56	Up	2.56
LPC20:3-b	POS	545.3484	546.3562	9.04	[M+H]+	9.24E-03	2.48E-02	3.28	Up	3.28
LPC20:4 b	POS	543.3313	544.3391	8.16	[M+H]+	5.10E-05	6.06E-04	13.05	Up	13.05
LPC20:5	POS	541.3151	542.3229	6.98	[M+H]+	3.84E-04	2.36E-03	8.83	Up	8.83
LPC22:5	POS	569.3492	570.357	8.69	[M+H]+	6.94E-04	3.44E-03	6.23	Up	6.23
LPC22:6-a	POS	567.3307	568.3385	7.74	[M+H]+	1.06E-02	2.76E-02	3.23	Up	3.23
LPC22:6-b	POS	567.331	568.3388	8.1	[M+H]+	2.02E-04	1.51E-03	6.64	Up	6.64
LPE20:4-b	POS	501.2852	502.293	8.37	[M+H]+	1.85E-03	7.01E-03	4.90	Up	4.90
LPE22:6-b	POS	525.2839	526.2917	8.3	[M+H]+	3.46E-03	1.13E-02	4.73	Up	4.73
PC(15:0_20:4)	POS	767.5452	768.553	20.38	[M+H]+	9.42E-09	1.98E-06	4.45	Up	4.45
PC(15:0_22:6)	POS	791.5451	792.5529	19.75	[M+H]+	4.96E-05	5.97E-04	2.32	Up	2.32
PC(16:0_15:0)	POS	719.546	720.5538	22.71	[M+H]+	2.04E-06	6.87E-05	2.65	Up	2.65
PC(16:0_16:0)	POS	733.5607	734.5685	24.62	[M+H]+	2.38E-05	3.60E-04	2.50	Up	2.50
PC(16:0_20:4n-3)	POS	781.5604	782.5682	22.13	[M+H]+	9.12E-09	1.98E-06	4.74	Up	4.74
PC(16:0_20:5)	POS	779.5448	780.5526	19.99	[M+H]+	6.70E-08	7.05E-06	3.15	Up	3.15
PC(16:0_22:4)	POS	809.5916	810.5994	24.9	[M+H]+	6.60E-05	6.98E-04	2.71	Up	2.71
PC(16:0_22:5)	POS	807.5757	808.5835	23.56	[M+H]+	3.26E-08	4.65E-06	3.75	Up	3.75
PC(17:0_20:4n-3)	POS	795.5773	796.5851	23.99	[M+H]+	3.34E-09	1.98E-06	4.15	Up	4.15
PC(17:0_22:6)	POS	819.5757	820.5835	23.26	[M+H]+	7.25E-07	3.37E-05	2.14	Up	2.14
PC(17:1_20:4)	POS	793.5606	794.5684	20.99	[M+H]+	1.85E-04	1.42E-03	3.03	Up	3.03
PC(18:0_20:4)	POS	809.5941	810.6019	25.9	[M+H]+	4.05E-08	5.16E-06	5.33	Up	5.33
PC(18:0_22:5n-3)	POS	835.6064	836.6142	26.29	[M+H]+	8.29E-09	1.98E-06	2.98	Up	2.98
PC(18:0_22:6)	POS	833.5905	834.5983	25.12	[M+H]+	3.68E-08	4.95E-06	2.72	Up	2.72
PC(18:1_22:5)	POS	833.5923	834.6001	23.08	[M+H]+	1.21E-07	9.80E-06	2.83	Up	2.83
PC(19:0_20:4)	POS	823.6086	824.6164	27.85	[M+H]+	3.77E-05	4.99E-04	2.04	Up	2.04
PC(20:1_22:6)	POS	859.6084	860.6162	25.52	[M+H]+	2.08E-04	1.53E-03	2.23	Up	2.23
PC(22:3_18:0)	POS	839.6394	840.6472	31.55	[M+H]+	5.87E-05	6.55E-04	2.91	Up	2.91
PC(18:1_22:6)	POS	831.5771	832.5849	21.97	[M+H]+	4.43E-07	2.66E-05	2.59	Up	2.59
PC(36:5)	POS	779.5452	780.553	19.35	[M+H]+	3.05E-07	2.00E-05	3.22	Up	3.22
PC(36:6)	POS	777.529	778.5368	17.48	[M+H]+	3.23E-07	2.06E-05	2.19	Up	2.19
PC(37:5)	POS	793.5608	794.5686	21.73	[M+H]+	1.90E-07	1.44E-05	2.90	Up	2.90
PC(38:3)	POS	811.6094	812.6172	27.51	[M+H]+	2.61E-07	1.76E-05	2.66	Up	2.66
PC(38:4)-OH	POS	825.5867	826.5945	19.27	[M+H]+	2.23E-03	8.06E-03	2.23	Up	2.23
PC(38:4)	POS	809.5927	810.6005	24.21	[M+H]+	8.77E-06	1.85E-04	2.63	Up	2.63
PC(38:4)	POS	807.5778	808.5856	22.62	[M+H]+	8.51E-10	1.98E-06	4.94	Up	4.94
PC(38:6)	POS	805.5602	806.568	20.5	[M+H]+	7.80E-08	7.71E-06	4.47	Up	4.47
PC(39:5)	POS	821.5928	822.6006	24.43	[M+H]+	9.83E-08	9.15E-06	3.41	Up	3.41
PC(39:6)	POS	819.5757	820.5835	21.41	[M+H]+	4.42E-05	5.60E-04	2.06	Up	2.06
PC(39:6)	POS	819.5765	820.5843	22.18	[M+H]+	1.86E-04	1.42E-03	2.88	Up	2.88
PC(40:4)	POS	837.6233	838.6311	28.73	[M+H]+	1.02E-05	2.04E-04	2.41	Up	2.41
PC(40:6)	POS	833.5928	834.6006	23.93	[M+H]+	2.25E-03	8.09E-03	3.65	Up	3.65
PC(O-16:0/20:4)	POS	767.5803	768.5881	24.2	[M+H]+	1.08E-07	9.60E-06	4.43	Up	4.43
PC(O-16:1/22:5)	POS	791.5811	792.5889	24	[M+H]+	2.83E-08	4.28E-06	3.31	Up	3.31
PC(O-22:0/20:4)	POS	851.6757	852.6835	35.52	[M+H]+	1.04E-04	9.67E-04	2.70	Up	2.70
PC(O-36:5)	POS	765.5667	766.5745	21.88	[M+H]+	3.81E-05	5.01E-04	2.25	Up	2.25
PC(O-38:4)	POS	795.6114	796.6192	28.11	[M+H]+	9.39E-04	4.27E-03	2.17	Up	2.17
PE(O-16:0/22:6)	POS	749.535	750.5428	24.18	[M+H]+	3.28E-03	1.09E-02	2.40	Up	2.40
PS(38:4)	POS	811.5372	812.545	22.97	[M+H]+	1.30E-06	5.07E-05	3.08	Up	3.08
SM(d18:1/16:0)	POS	702.5663	703.5741	19.95	[M+H]+	3.32E-05	4.60E-04	2.04	Up	2.04
GlcCer(d18:1/16:0)	POS	699.5624	700.5702	21.05	[M+H]+	7.30E-05	7.59E-04	2.61	Up	2.61
CE20:4	POS	689.6104	690.6182	49.76	[M+NH4]+	2.62E-05	3.91E-04	2.33	Up	2.33
TG 53:4	POS	885.7803	886.7881	55.51	[M+NH4]+	8.84E-07	3.96E-05	3.92	Up	3.92
TG 53:5	POS	883.7684	884.7762	50.97	[M+NH4]+	1.00E-06	4.18E-05	4.52	Up	4.52
TG 54:5	POS	897.7802	898.788	52.78	[M+NH4]+	1.74E-04	1.37E-03	4.14	Up	4.14
TG 54:6	POS	895.7654	896.7732	49.98	[M+NH4]+	2.15E-06	7.02E-05	2.54	Up	2.54
TG 55:4	POS	913.8117	914.8195	62.21	[M+NH4]+	1.16E-04	1.04E-03	2.16	Up	2.16
TG 55:4	POS	913.8109	914.8187	60.2	[M+NH4]+	4.81E-08	5.54E-06	4.29	Up	4.29
TG 55:4	POS	913.8095	914.8173	63.62	[M+NH4]+	2.27E-07	1.62E-05	6.28	Up	6.28
TG 55:6	POS	909.7801	910.7879	49.95	[M+NH4]+	2.20E-05	3.49E-04	3.61	Up	3.61
TG 55:6	POS	909.7812	910.789	52.7	[M+NH4]+	5.59E-07	2.88E-05	6.47	Up	6.47
TG 55:7	POS	907.7659	908.7737	47.97	[M+NH4]+	2.00E-08	3.46E-06	3.42	Up	3.42
TG 56:3	POS	929.8412	930.849	79.24	[M+NH4]+	8.58E-06	1.83E-04	3.14	Up	3.14
TG 56:4	POS	927.827	928.8348	67.08	[M+NH4]+	1.53E-05	2.73E-04	3.61	Up	3.61
TG 56:4	POS	927.8244	928.8322	68.81	[M+NH4]+	2.18E-07	1.60E-05	5.91	Up	5.91
TG 56:5	POS	925.8109	926.8187	59.57	[M+NH4]+	5.45E-06	1.32E-04	8.54	Up	8.54
TG 54:3	POS	901.812	902.8198	66.65	[M+NH4]+	4.91E-07	2.66E-05	3.20	Up	3.20
TG 58:7	POS	949.8144	950.8222	56.2	[M+NH4]+	6.02E-09	1.98E-06	10.86	Up	10.86
TG(18:0_16:0_20:4)	POS	899.7958	900.8036	59.22	[M+NH4]+	3.55E-07	2.20E-05	5.27	Up	5.27
TG(18:1_16:0_22:5)	POS	923.7959	924.8037	52.64	[M+NH4]+	7.28E-09	1.98E-06	5.84	Up	5.84
TG(18:1_16:0_22:6)	POS	921.7813	922.7891	50.28	[M+NH4]+	1.17E-08	2.19E-06	5.09	Up	5.09
TG(18:1_16:0_24:5)	POS	951.8288	952.8366	58	[M+NH4]+	1.70E-07	1.33E-05	4.23	Up	4.23
TG(18:1_18:0_22:5)	POS	951.8276	952.8354	59.37	[M+NH4]+	5.76E-09	1.98E-06	7.57	Up	7.57

Supplemental Table 1. Primer sequences used for qPCR

Gene	Forward Sequence (5'-3')	Reverse Sequence (5'-3')
Ywhab	AATGCCACCCAGGCAGAAAGCA	CTTGGTAAGCCTGCTGGGAGTT
Ywhag	GGACTATTACCGTTACCTGGCAG	CTGCATGTGCTCCTTGCTGATC
Ywhae	CTAACACTGGCGAGTCCAAGGT	GTAAGCCACGAGGCTGTTCTCT
Ywhah	CCGCGTATAAGGAAGCCTTCGA	AGGCTTGCTCTGGTGCATTCTG
Ywhas	CATGAAGAGCGCCGTGGAAAAG	CTCTTCTGCTCGATGCTGGACA
Ywhaq	GCTGAAGTAGCTTGTGGCGATG	ATGCGTAGGCTGCATCTCCTTC
Ywhaz	CAGAAGACGGAAGGTGCTGAGA	CTTTCTGGTTGCGAAGCATTGGG
Hprt1	TCCTCCTCAGACCGCTTTT	CCTGGTTCATCATCGCTAATC
Adrb1	CTCGTCCGTCGTCTCCTTCTAC	GTCGATCTTCTTTACCTGTTTTTGG
Adrb2	TTGCAGTGGATCGCTATGTTG	TGACCACTCGGGCCTTATTCT
Adrb3	CCTTCAACCCGGTCATCTAC	GAAGATGGGGATCAAGCAAGC
Pde3b	CTTCACAAGGGATTGAGTGGCAGAACC	CATCCATGACTTGAAACACTGACTTCTTGG
Pde4a	TGGATGCCGTGTTCACAGACCTGG	GTTCTCAAGCACAGACTCATCGTTGTAC
Pde4b	CAGGAAAATGGTGATTGACATGGTGTTGG	CGAAGAACCTGTATCCGGTCAGTATAG
Pde4d	GGTCATTGACATTGTCCTGGCGACAG	CAGTGCACCATATTCTGAAGGACCTGG
Pparg	GGTCAGCTCTTGTGAATGGAA	ATCAGCTCTGTGGACCTCTCC
Fabp4	AGTACTCTCTGACCGGATGG	GGAAGCTTGTCTCCAGTGAA
Fasn	TGGGTTCTAGCCAGCAGAGT	ACCACCAGAGACCGTTATGC
Atgl	AACACCAGCATCCAGTTCAA	GGTTCAGTAGGCCATTCCTC
Hsl	ACCGAGACAGGCCTCAGTGTG	GAATCGGCCACCGGTAAAGAG
Magl	GTGCCTACCTGCTCATGGAAT	GAGGACGGAGTTGGTCACTTC
Lpl	GTGACCGATTTCATCAAGTTTGGAG	GACGGACACAAAGTTAGCACCAC

Supplemental table 2: Antibodies used

Target	Host species	Dilution	Source	Product ID	RRID
Phosphorylated HSL (S660)	Rabbit	1:1000	Cell Signaling Technology	4126	AB_490997
HSL	Rabbit	1:1000	Cell Signaling Technology	4107	AB_2296900
Phosphorylated CREB (S133)	Rabbit	1:1000	Cell Signaling Technology	9198	AB_2561044
CREB	Rabbit	1:1000	ThermoFisher	MA1-083	AB_558523
ATGL	Rabbit	1:1000	Cell Signaling Technology	2439	AB_2167953
PPARγ	Rabbit	1:1000	Cell Signaling Technology	2443	AB_823598
β-actin	Mouse	1:1000	Cell Signaling Technology	3700	AB_2242334
β-tubulin	Mouse	1:1000	Cell Signaling Technology	86298	AB_2715541
Anti-rabbit IgG HRP-linked antibody	Goat	1:2000	Cell Signaling Technology	7074	AB_2099233
Anti-mouse IgG HRP-linked antibody	Goat	1:5000	Cell Signaling Technology	7076	AB_330924
14-3-3ζ	Rabbit	1:1000	Cell Signalling Technology	7413	AB_10950820
14-3-3ζ	Abcam	1:!00	Abcam	Ab51129	AB_867447
Perilipin	Rabbit	1:1000	Cell Signaling Technology	9349	AB_10829911
Perilipin	Guinea pig	1:1500	Fitzgerald	20R-PP004	AB_1288416

Figure 1

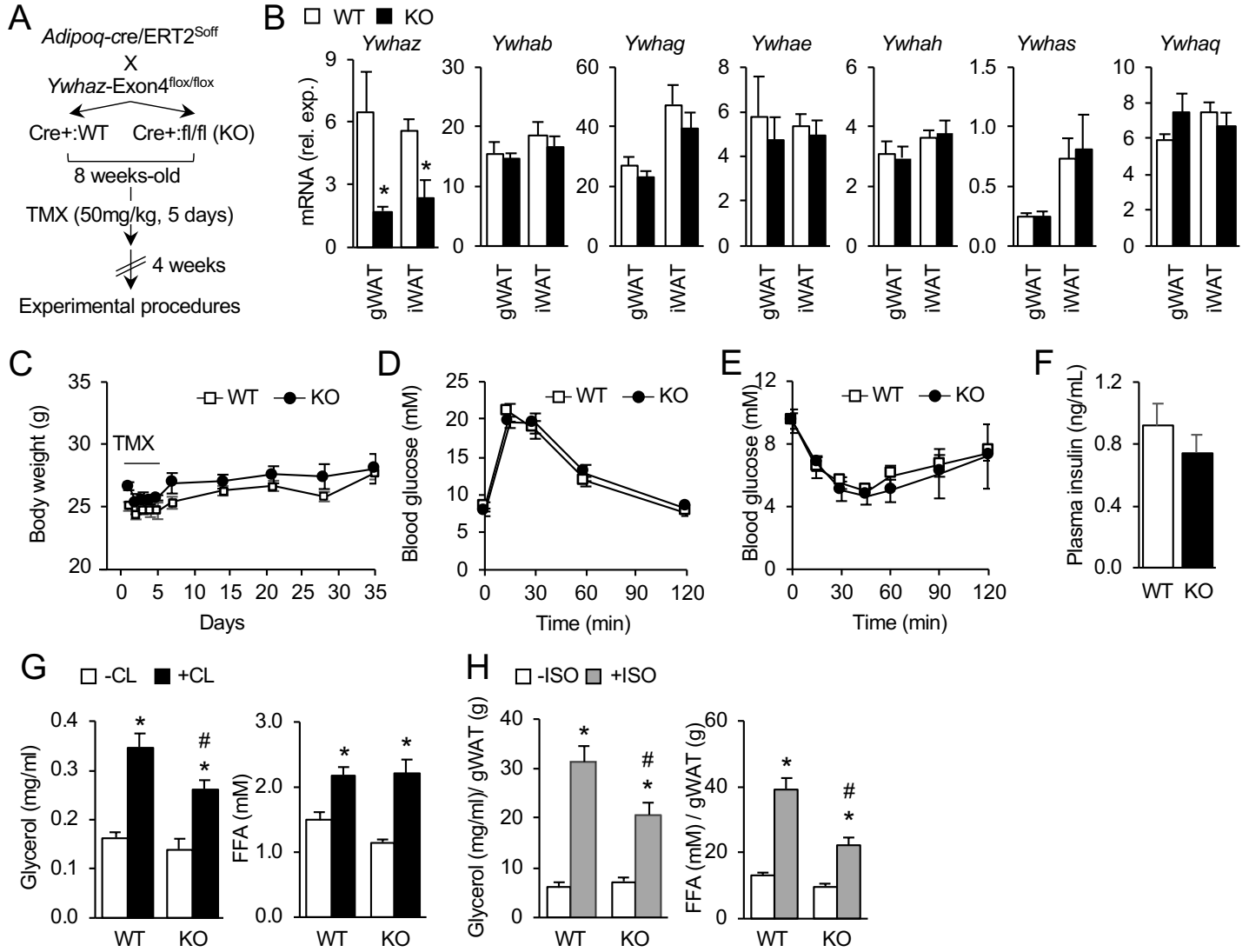

Figure 2

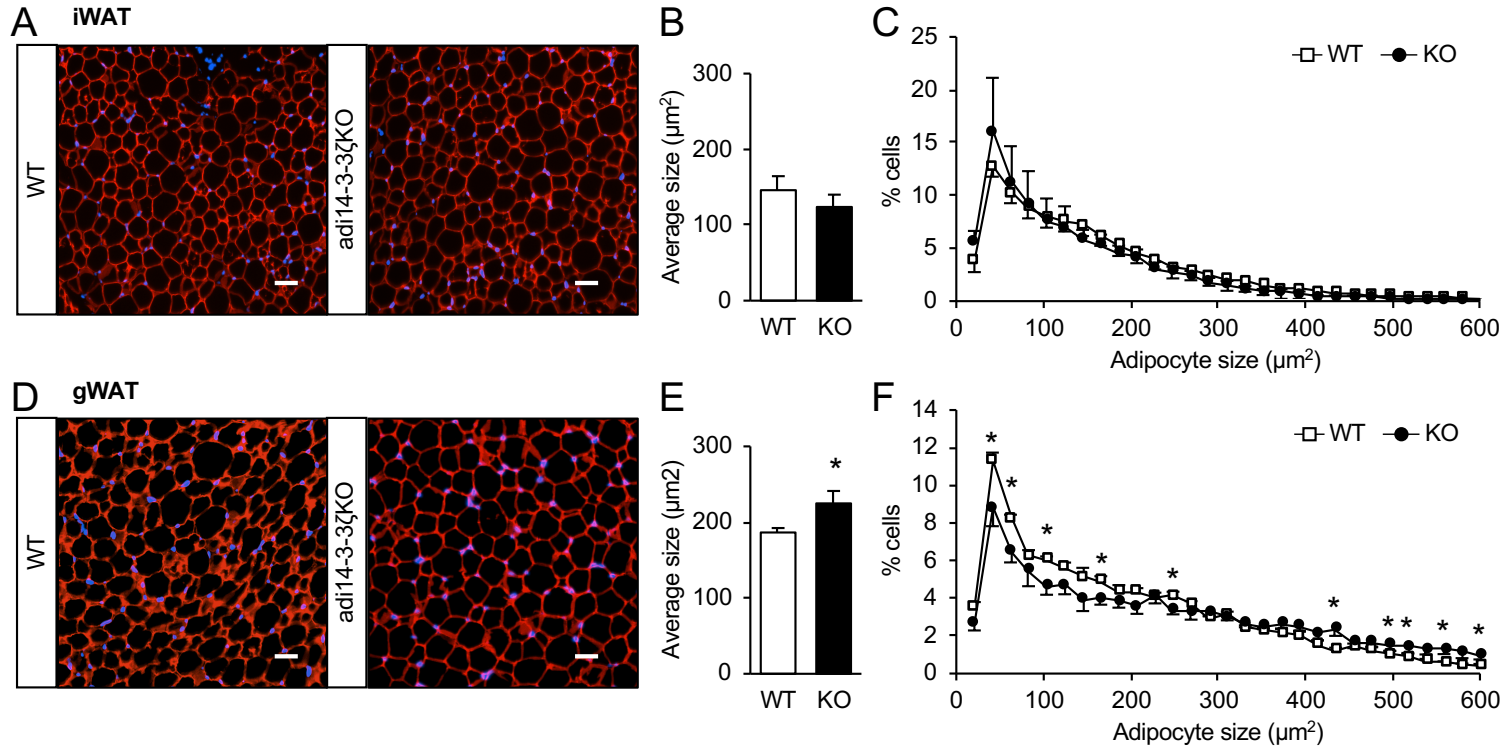

Figure 3

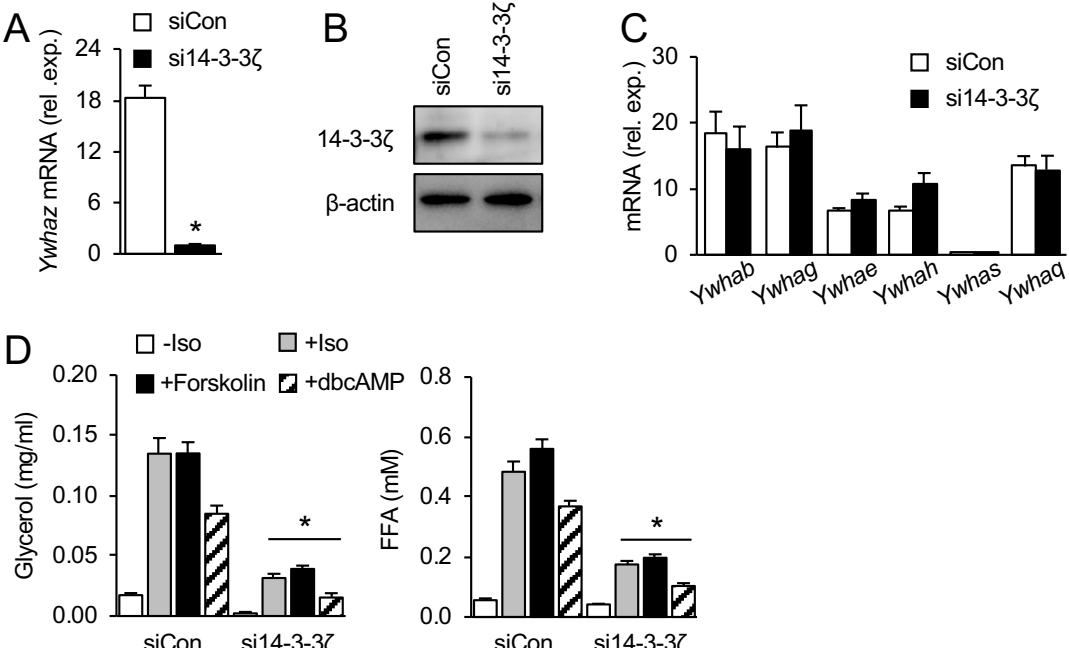

Figure 4

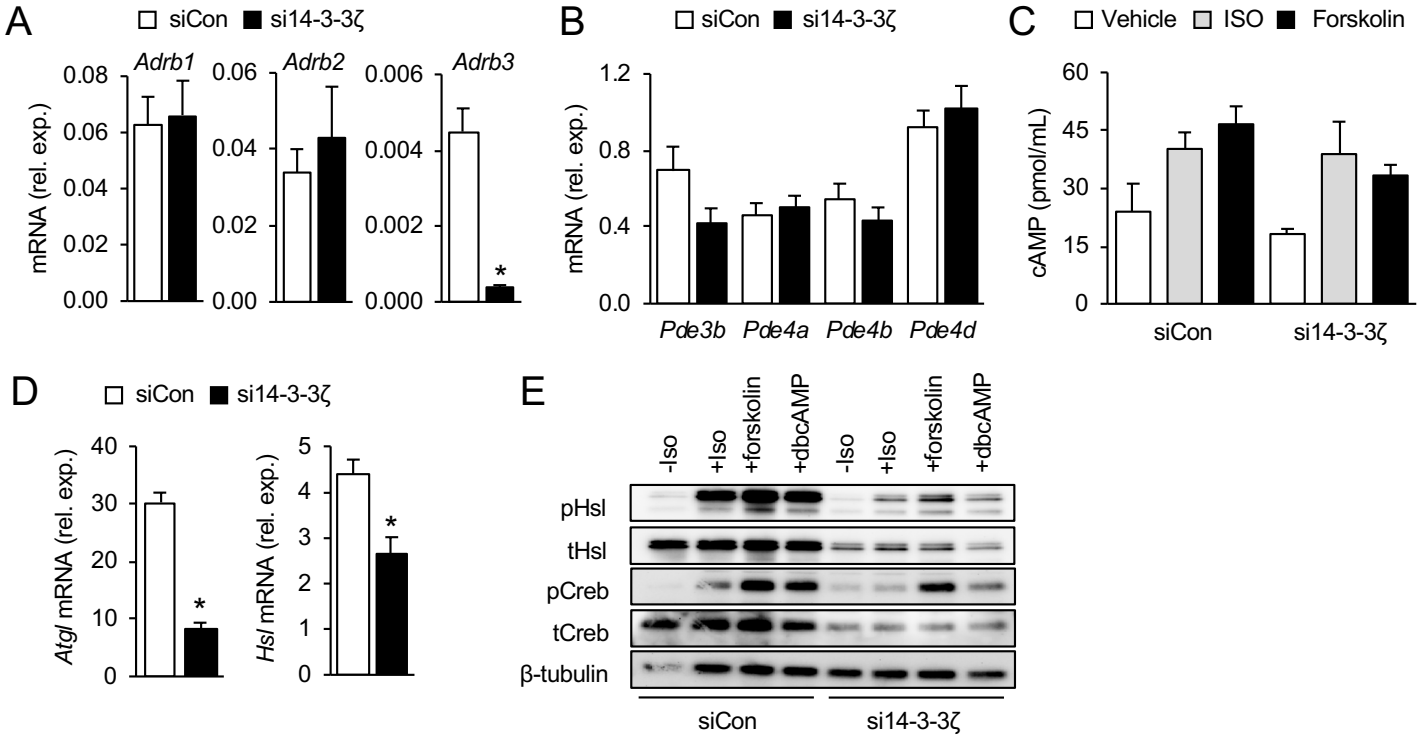

Figure 5

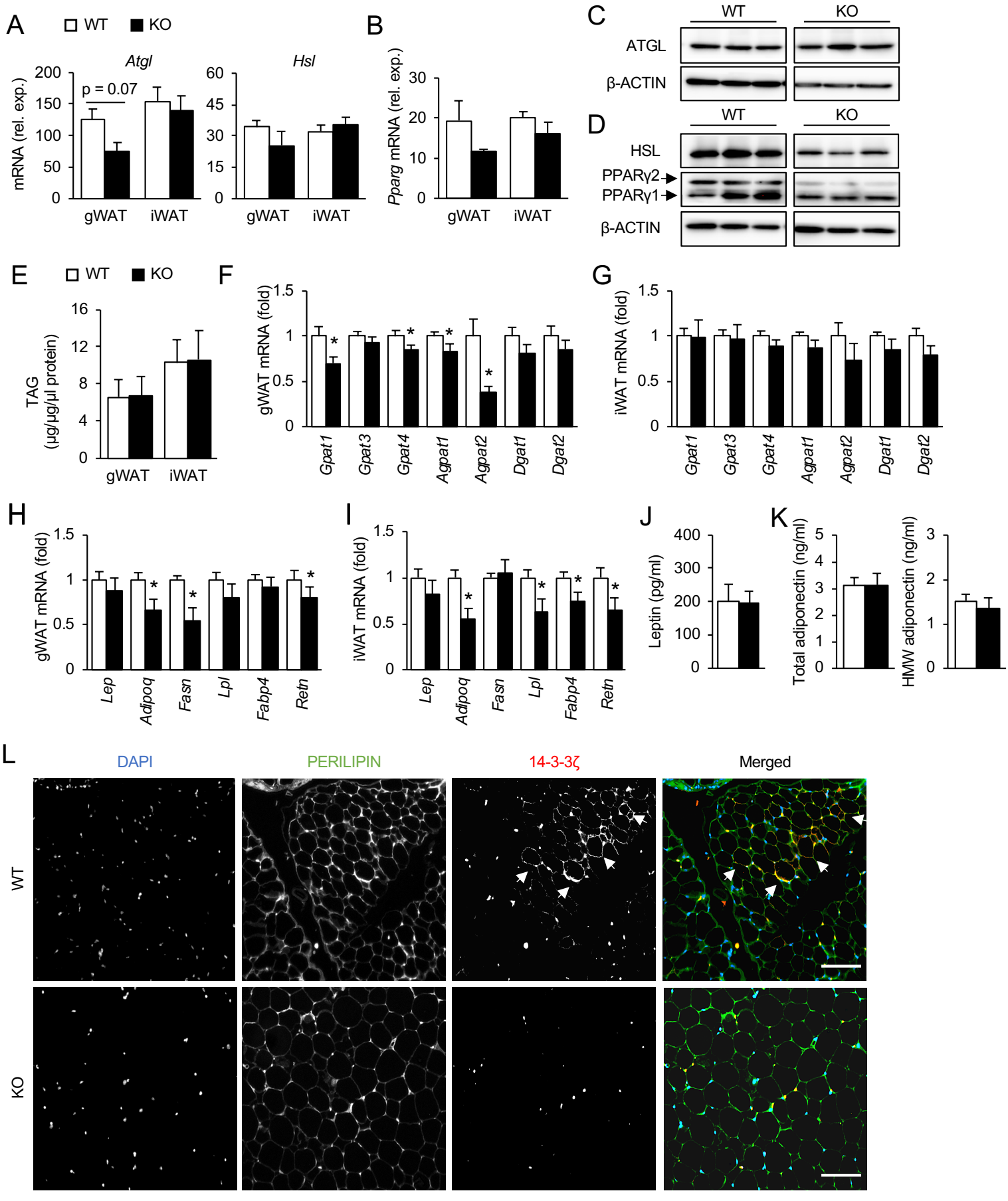

Figure 6

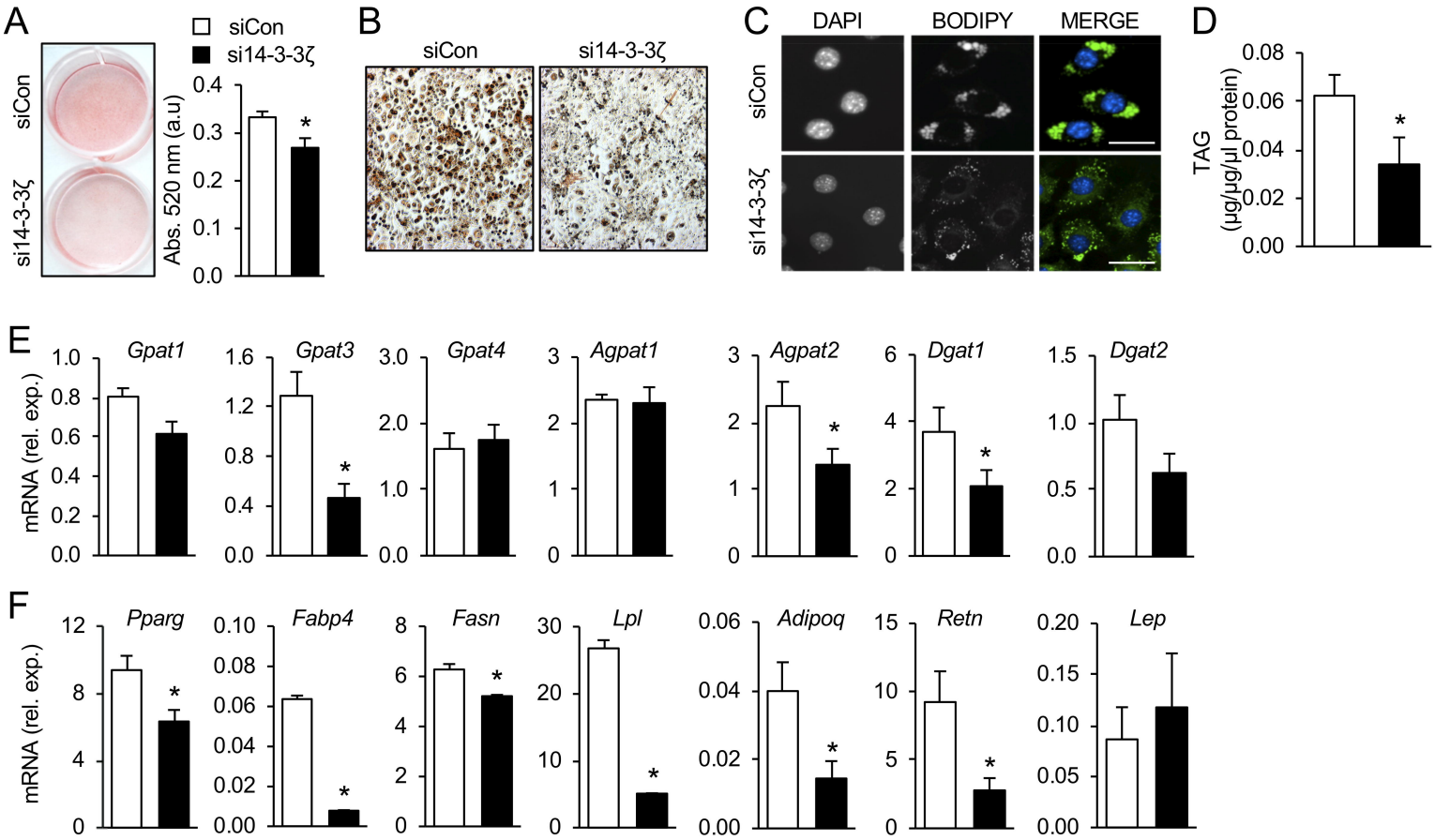
A
siCon
si14-3-3ζ
siCon
si14-3-3ζ
Abs. 520 nm (a.u)
0.4
0.3
0.2
0.1
0.0
*
B
siCon
si14-3-3ζ
C
DAPI
BODIPY
MERGE
siCon
si14-3-3ζ
D
TAG
(μg/μg/μl protein)
0.08
0.06
0.04
0.02
0.00
*
E
mRNA (rel. exp.)
Gpat1
1.0
0.8
0.6
0.4
0.2
0.0
Gpat3
1.6
1.2
0.8
0.4
0.0
*
Gpat4
3.0
2.0
1.0
0.0
Agpat1
3
2
1
0
Agpat2
3
2
1
0
*
Dgat1
6
4
2
0
*
Dgat2
1.5
1.0
0.5
0.0
F
mRNA (rel. exp.)
Pparg
12
8
4
0
*
Fabp4
0.10
0.08
0.06
0.04
0.02
0.00
*
Fasn
8
6
4
2
0
*
Lpl
30
20
10
0
*
Adipoq
0.06
0.04
0.02
0.00
*
Retn
15
10
5
0
*
Lep
0.20
0.15
0.10
0.05
0.00

Figure 7

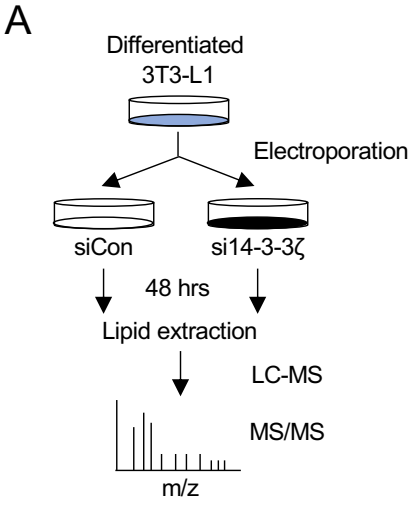

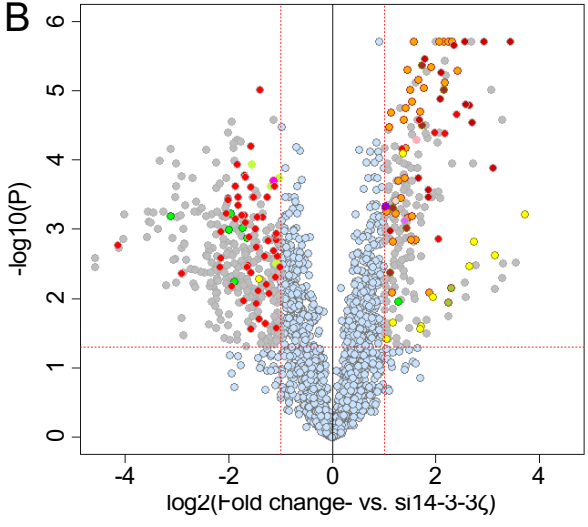

Lipid Class	Up Regulated	Down Regulated
LPC	10	1
PC	31	-
PC(O)	5	-
PC-OH	1	-
LPE	2	-
PE	-	4
PE(O)	1	6
PI	-	1
PS	1	-
Sphingomyelin	1	-
GlcCeramide	1	-
Cholesteryl Ester	1	-
TG (<54 carbons)	2	52
TG (>54 carbons)	19	-
Unknown